2006

Rab22a regulates the sorting of transferrin to recycling endosomes

Javier G. Magadan
Washington University School of Medicine in St. Louis
M. Alejandro Barbieri
Washington University School of Medicine in St. Louis
Rosana Mesa
Universidad Nacional de Cuyo
Philip D. Stahl
Washington University School of Medicine in St. Louis
Luis S. Mayorga
Universidad Nacional de Cuyo

Molecular and Cellular Biology

Rab22a Regulates the Sorting of Transferrin to Recycling Endosomes

Javier G. Magadán, M. Alejandro Barbieri, Rosana Mesa, Philip D. Stahl and Luis S. Mayorga
Mol. Cell. Biol. **2006, 26(7):2595. DOI: 10.1128/MCB.26.7.2595-2614.2006.**

MOLECULAR AND CELLULAR BIOLOGY, Apr. 2006, p. 2595–2614 Vol. 26, No. 7
0270-7306/06/$08.00+0 doi:10.1128/MCB.26.7.2595–2614.2006

Rab22a Regulates the Sorting of Transferrin to Recycling Endosomes‡

Javier G. Magadán,[1,2] M. Alejandro Barbieri,[2]† Rosana Mesa,[1] Philip D. Stahl,[2] and Luis S. Mayorga[1]*

Laboratorio de Biología Celular y Molecular, Instituto de Histología y Embriología (IHEM-CONICET), Facultad de Ciencias Médicas, Universidad Nacional de Cuyo, 5500 Mendoza, Argentina,[1] and Department of Cell Biology and Physiology, Washington University School of Medicine, St. Louis, Missouri 63110[2]

Received 8 August 2005/Returned for modification 1 September 2005/Accepted 13 January 2006

Rab22a is a member of the Rab family of small GTPases that localizes in the endocytic pathway. In CHO cells, expression of canine Rab22a (cRab22a) causes a dramatic enlargement of early endocytic compartments. We wondered whether transferrin recycling is altered in these cells. Expression of the wild-type protein and a GTP hydrolysis-deficient mutant led to the redistribution of transferrin receptor to large cRab22a-positive structures in the periphery of the cell and to a significant decrease in the plasma membrane receptor. Kinetic analysis of transferrin uptake indicates that internalization and early recycling were not affected by cRab22a expression. However, recycling from large cRab22a-positive compartments was strongly inhibited. A similar effect on transferrin transport was observed when human but not canine Rab22a was expressed in HeLa cells. After internalization for short periods of time (5 to 8 min) or at a reduced temperature (16°C), transferrin localized with endogenous Rab22a in small vesicles that did not tubulate with brefeldin A, suggesting that the endogenous protein is present in early/sorting endosomes. Rab22a depletion by small interfering RNA disorganized the perinuclear recycling center and strongly inhibited transferrin recycling. We speculate that Rab22a controls the transport of the transferrin receptor from sorting to recycling endosomes.

Most macromolecules internalized by clathrin-dependent and -independent endocytosis are delivered to sorting endosomes, a dynamic tubovesicular compartment with a central role in the targeting of material to different intracellular destinations (10). Within this compartment, a first segregation of membrane-bound from soluble molecules occurs by geometrical means. The narrow tubules pinching off from sorting endosomes are enriched in membrane-associated molecules because of their large area-to-volume ratio. In contrast, soluble molecules (e.g., ligands dissociated from their receptors at the low pH of endosomes) accumulate in the vesicular portion of sorting endosomes. Most of the material associated with tubules is either transported back to the plasma membrane or transferred to the recycling compartment. In contrast, most of the soluble material is delivered to late endosomes. Membrane invaginations in the sorting endosomes form intraluminal vesicles that are also targeted to late endosomes, providing an efficient route to digest transmembrane proteins (e.g., receptors that need to be down-regulated) (7, 25). Sorting, late, and recycling endosomes also exchange macromolecules with the exocytic pathway, mostly with the *trans*-Golgi network (TGN) (10). The active interaction between endocytic compartments and the cytoskeleton promotes the pinching off of tubular structures and contributes to the positioning of organelles within the cell (15). Sorting endosomes are found principally in the periphery of the cell, whereas late endosomes and recycling endosomes are more prominent in the perinuclear region. The organization of lipid-protein domains containing specific sets of macromolecules in the membrane of sorting endosomes provides an additional layer of selectivity for the differential targeting of membrane-bound compartments derived from sorting endosomes to specific destinations (18).

The small GTPases of the Rab family are active protagonists in the transport of macromolecules along the endocytic and exocytic pathways. Rabs participate in vesicle budding and interaction with the cytoskeleton. However, the best-characterized function of these GTPases is in membrane fusion, where they have an active role in tethering the compartments that are going to fuse (17). Lately, it has been recognized that Rabs participate in the organization of membrane domains in membrane-bound compartments (29). Therefore, the presence of several Rabs with overlapping distribution in sorting and recycling endosomes is not surprising. Rab5 associates with the plasma membrane and sorting endosomes and is necessary at early steps in the endocytic pathway (2). Direct recycling of receptors from these vesicles to the plasma membrane requires Rab4 (4), while recycling via the perinuclear recycling center depends on Rab11 (26). Kinetic studies of living cells indicate that proteins following the recycling pathway associate early after internalization with Rab5-positive structures. Afterward, the internalized markers move first to Rab4- and later to Rab11-containing compartments. Most compartments along this route contain more than one Rab, frequently segregated in different domains (24). Compartments containing Rab5 and Rab4 or Rab4 and Rab11 have been described previously (24, 27). According to recent reports, Rab11 participates in the most distal event of this pathway, the fusion of recycling endosomes with the plasma membrane (27).

Rab22a is another member of the Rab family that localizes in the endocytic pathway (12, 13, 9). Canine Rab22a (cRab22a) colocalizes extensively with Rab5 and physically interacts with the early endosomal antigen 1 (EEA1), one of the best-char-

* Corresponding author. Mailing address: Instituto de Histología y Embriología (IHEM-CONICET), Casilla de Correo 56, 5500 Mendoza, Argentina. Phone: 54-261-4494143. Fax: 54-261-4494117. E-mail: lmayorga@fcm.uncu.edu.ar.

† Present address: Department of Biological Sciences, Florida International University, University Park, Miami, FL 33199.

‡ Supplemental material for this article may be found at http://mcb.asm.org/.

acterized effectors of Rab5 (9). In CHO cells, expression of green fluorescent protein (GFP)-tagged cRab22a causes a dramatic enlargement of sorting endosomes and delays the transport of cholera toxin and cation-independent mannose-6-phosphate receptor to the TGN (12). In contrast, transport to lysosomes is not significantly affected. In HeLa cells, expression of this protein alters the recycling of the major histocompatibility complex class I (MHC-I) to the cell surface. In contrast, the recycling of transferrin (Tfn) is not affected (28). However, we have observed that Tfn accumulates in cRab22a-containing compartments in CHO cells. The aim of the present work was to characterize the function of Rab22a in the Tfn recycling pathway. The results indicate that expression of the Rab22a wild type or a GTPase-deficient mutant prevents the transport of Tfn and its receptor to recycling endosomes in CHO and HeLa cells. As a consequence, the recycling of Tfn is strongly diminished. We observed that Tfn localizes with endogenous Rab22a in early/sorting endosomes and that partial depletion of the protein significantly inhibits Tfn recycling.

MATERIALS AND METHODS

Cell culture. Media and reagents for cell culture were purchased from GIBCO BRL (Eggenheim, Germany). TRVb-1 is a CHO cell line that does not express endogenous hamster Tfn receptor (TfnR) and has been transfected with human TfnR (11). HeLa, HEK 293, and Vero cells were grown in Dulbecco's modified Eagle's medium, TRVb-1 in Ham's F-12 medium, and BHK-21 in α-minimal essential medium, each supplemented with 10% heat-inactivated fetal bovine serum (FBS), 100 U/ml penicillin, 100 μg/ml streptomycin, and 2 mM L-glutamine at 37°C in a humidified atmosphere of 5% carbon dioxide in air. TRVb-1 cells were maintained under selection in the above-described medium containing 400 μg/ml G-418.

Antibodies. Mouse monoclonal anti-human TfnR antibody was purchased from Zymed Laboratories Inc. (San Francisco, CA). Mouse monoclonal anti-α-tubulin antibody was obtained from Sigma Chemical Co. (St. Louis, MO). Mouse monoclonal anti-EEA1 antibody was from BD Transduction Laboratories (Lexington, KY). Mouse monoclonal anti-lysobisphosphatidic acid (LBPA) antibody was a generous gift from Jean Gruenberg (Department of Biochemistry, University of Geneva, Geneva, Switzerland). Rabbit polyclonal anti-cathepsin D antibody was kindly provided by William Brown (Section of Biochemistry, Molecular and Cell Biology, Cornell University, Ithaca, NY). Alexa Fluor (546 or 488)-conjugated goat anti-mouse or anti-rabbit immunoglobulin G (heavy plus light chains) was from Molecular Probes (Eugene, OR). Peroxidase AffiniPure goat anti-mouse or anti-rabbit immunoglobulin G (heavy plus light chains) was from Jackson ImmunoResearch Laboratories Inc. (West Grove, PA).

Production of purified polyclonal anti-Rab22a antibody. The peptide PSG GKGFKLRRQPSEP corresponding to a sequence of amino acids present in the carboxy termini of canine and human Rab22a was conjugated to keyhole limpet hemocyanin via a cysteine group added to the amino-terminal end of the peptide. Rabbits were immunized with the conjugate, and the serum was collected (Genemed Synthesis Inc., San Francisco, CA). The antibody was affinity purified using the peptide immobilized in an Affi-Gel 10 column (Sigma Chemical Co.).

siRNA-mediated depletion of human Rab22a. The pSuper.gfp/neo vector (OligoEngine, Seattle, WA) (1) was used to produce small interfering RNA (siRNA) molecules in transfected HeLa cells. The target sequence for the human Rab22a chosen was previously described to knock down this protein in HeLa cells (28). A 60-nucleotide-long double-stranded DNA insert containing the human Rab22a (hRab22a) sequence (5′-AAGGACTACGCCGACTCTA-3′) as an inverted repeat separated by a 9-nucleotide-long hairpin region was generated by annealing two complementary sequences. As a control, a 19-nucleotide scrambled oligonucleotide was replaced by the hRab22-specific sequence. The double-stranded DNAs were inserted into the BglII/XhoI site of the pSuper.gfp/neo plasmid. Transient transfections were carried out using 1 μg of DNA and 3 μl of Lipofectamine 2000 (Invitrogen Argentina S.A., Buenos Aires, Argentina) for 24-well culture plates, according to the instructions supplied by the manufacturer.

Plasmids and viruses. The cDNA for canine Rab22a was kindly provided by Marino Zerial (Max Planck Institute for Molecular Cell Biology and Genetics, Dresden, Germany). The cRab22a wild-type and Q64L mutant sequences were subcloned into the BamHI site of the pEGFP-C1 vector (Clontech, Palo Alto, CA). The human cDNA clone containing the open reading frame for Rab22a (BC063457/IMAGE, 5182786) was obtained from the American Type Culture Collection (Manassas, VA). The human Rab22aQ64L mutant was obtained by site-directed mutagenesis (QuikChange kit; Stratagene, La Jolla, CA). The mutations were verified by sequencing the insert. The human wild-type and Q64L mutant sequences were subcloned by PCR into the BamHI site of the pEGFP-C1 vector. The plasmid pERFP-cRab22aWT was constructed by subcloning canine Rab22aWT into the BamHI site of the pERFP plasmid following standard procedures. For transient expression of GFP-human Rab5aWT, the cDNA was amplified by PCR from pUC-hRab5aWT and subcloned as a HindIII-BamHI fragment into a pEGFP-C1 vector. The plasmid pCMV-EGFP-C3-human Rab4a was kindly provided by Ira Mellman (Yale University School of Medicine, New Haven, CT). The plasmid pEGFP-C1-human Rab11aWT was a generous gift of María Isabel Colombo (IHEM-CONICET, Facultad de Ciencias Médicas, Universidad Nacional de Cuyo, Mendoza, Argentina). The original hRab11aWT cDNA was from David Sabatini (Department of Cell Biology and Kaplan Cancer Center, New York University School of Medicine, NY). The plasmid pEGFP-C3-human cellubrevin was generously provided by Thierry Galli (Membrane Traffic and Neuronal Plasticity, Institut du Fer-à-Moulin, Paris, France). Transient transfections were carried out using 1 μg of DNA and 3 μl of FuGENE 6 (Roche Applied Science, Indianapolis, IN) for 24-well culture plates, according to the instructions supplied by the manufacturer. Experiments were performed 18 h after transfection. For colocalization studies in double transfection experiments, all cRab22a-positive vesicles were counted in a single confocal plane in at least 10 cells with low levels of expression. These vesicles (a total of about 3,000) were classified according to whether they contained the other fluorescent protein. Results are expressed as percentages of cRab22a-positive structures containing both proteins.

Canine Rab22a wild-type and Rab22aQ64L cDNAs from pEGFP-C1 were subcloned into the XbaI site of the Sindbis expression vector pTOTO3′2J1. The correct sequence and orientation of the inserts were confirmed by DNA sequencing. The recombinant Sindbis viruses (called 2JC1) were produced by Lipofectin-mediated transfection (Invitrogen, Carlsbad, CA) of BHK-21 cells by using capped RNAs derived from SP6 RNA polymerase transcription of XhoI-linearized plasmid templates. The viruses in the medium were harvested 40 h after transfection. Virus titers were generally between 10^8 and 10^9 PFU/ml. Virus stocks were aliquoted and kept frozen at −80°C before use.

Indirect immunofluorescence experiments. Cells on 12-mm round glass coverslips were washed three times with ice-cold phosphate-buffered saline (PBS)–Ca^{2+}/Mg^{2+} (PBS, 1 mM $MgCl_2$, and 1 mM $CaCl_2$) and fixed with 3% paraformaldehyde and PBS-Ca^{2+}/Mg^{2+} solution at room temperature for 15 min. After three 5-min PBS-Ca^{2+}/Mg^{2+} washes, the cells were permeabilized in 0.05% saponin, 0.2% bovine serum albumin (BSA), and PBS-Ca^{2+}/Mg^{2+} for 15 min at room temperature. The cells were washed three times for 5 min with 0.05% saponin, 0.2% BSA, and PBS-Ca^{2+}/Mg^{2+}, and the free aldehyde groups were quenched at room temperature for 25 min with 0.05% saponin, 50 mM NH_4Cl, 0.2% BSA, 1% goat serum, and PBS-Ca^{2+}/Mg^{2+} solution. To immunostain compartments containing human TfnR, EEA1, LBPA, cathepsin D, or Rab22a, cells were incubated with the corresponding primary antibody (20 μg/ml for the anti-Rab22a antibody and 5 μg/ml for the others) in blocking buffer (0.05% saponin, 0.2% BSA, 1% goat serum, and PBS-Ca^{2+}/Mg^{2+}) overnight at 4°C. Unbound primary antibody was removed with three 5-min washes with 0.05% saponin, 0.2% BSA, and PBS-Ca^{2+}/Mg^{2+}, and the coverslips were incubated with the appropriate secondary antibody (conjugated to Alexa Fluor 546 or 488) diluted 1/250 (or 1/750 for Rab22a immunostaining) in blocking buffer for 1 h at room temperature. Cells were subjected to three 5-min washes with 0.05% saponin, 0.2% BSA, and PBS-Ca^{2+}/Mg^{2+}, rinsed in Millipore water for 5 min, and mounted on coverslip slides using a ProLong Antifade kit (Molecular Probes).

Fluorescent Tfn internalization studies. TRVb-1, HeLa, HEK 293, Vero, and BHK-21 cells were grown on coverslips and preincubated in internalization medium (serum-free medium containing 2 mg/ml BSA and 20 mM NaOH and HEPES [pH 7.4]) for 60 min at 37°C, immediately prior to uptake experiments to deplete endogenous Tfn. For continuous uptake, the cells were incubated at 37°C for 30 min in internalization medium containing 40 μg/ml tetramethylrhodamine- or Alexa Fluor 647-conjugated human Tfn (Molecular Probes). When indicated, the uptake was performed for 90 min at 16°C. For surface binding, the cells were incubated with 40 μg/ml tetramethylrhodamine-conjugated human Tfn in internalization medium for 90 min on ice. After Tfn internalization or surface binding, the cells were washed extensively in ice-cold 0.5% BSA and PBS, and the probe was chased at 37°C for different time periods in the presence of a 100-fold excess of unlabeled iron-saturated human Tfn (Calbiochem, San Diego,

CA) and 100 μM deferoxamine mesylate (Sigma Chemical Co.) to prevent fluorescent Tfn reinternalization. At the end of each time point, surface-bound fluorescent Tfn was stripped by washing the cells three times alternately in ice-cold 0.1% BSA and PBS and 0.1% BSA, 25 mM glacial acetic acid, and PBS (pH 4.2). The coverslips were rinsed briefly in ice-cold PBS-Ca^{2+}/Mg^{2+} and fixed with 3% paraformaldehyde and PBS-Ca^{2+}/Mg^{2+} solution. After three 5-min washes with PBS-Ca^{2+}/Mg^{2+}, the cells were incubated with 50 mM NH_4Cl in PBS-Ca^{2+}/Mg^{2+} at room temperature for 15 min and processed for confocal fluorescence microscopy. For quantification, the Tfn-associated fluorescence (summation of all confocal planes, background subtracted) was measured in 20 cells using ImageJ free image analysis software (http://rsb.info.nih.gov/ij/; W. Rasband, National Institutes of Health, Bethesda, MD) and expressed in arbitrary units/cell. For time course experiments, the results are expressed as percentages of fluorescence/cell observed before chasing (i.e., after the 30-min internalization or after the 4°C binding). For colocalization studies, all Rab22a-positive vesicles were counted in at least 10 cells for each time point. These vesicles (a total of about 2,000) were classified according to whether they contained Tfn. Results are expressed as percentages of Rab22a-positive structures that contained Tfn.

Labeling of acidic compartments. The acidotropic dye LysoTracker Red DND-99 (Molecular Probes) was diluted from a 1 mM stock solution to the final working concentration (75 nM) in internalization medium. For labeling acidic compartments, TRVb-1 living cells were incubated with the probe for 30 min at 37°C. After incubation, the coverslips were washed extensively with ice-cold PBS-Ca^{2+}/Mg^{2+}, fixed with 3% paraformaldehyde and PBS-Ca^{2+}/Mg^{2+} solution, and processed for confocal fluorescence microscopy.

Bf treatment. Brefeldin A (BfA; Sigma Chemical Co.) was dissolved in absolute ethanol at 5 mg/ml stock solution and stored at −20°C. HeLa or TRVb-1 cells were pretreated for 15 min at 37°C with 5 μg/ml BfA in internalization medium and then continuously labeled with 40 μg/ml tetramethylrhodamine- or Alexa Fluor 647-conjugated human Tfn for 30 min at 37°C in the presence of the drug.

Scanning laser confocal microscopy. The cells were examined with a Nikon C1 laser scanning confocal unit (Nikon D-Eclipse C1) attached to an upright fluorescence microscope (Nikon Eclipse E600) with a 63×, 1.4 Plan Apochromat objective (Nikon). The images were collected by using separate filters for each fluorochrome viewed (Alexa Fluor 488 and GFP, $\lambda_{excitation}$ = 488 nm and $\lambda_{emission}$ = 515 nm; tetramethylrhodamine and Alexa Fluor 546, $\lambda_{excitation}$ = 568 nm and $\lambda_{emission}$ = 585 nm). Images were acquired digitally and processed using the operation software EZ-C1 for the Nikon C1 confocal microscope. Labeled cells with Alexa Fluor 647 fluorophore were analyzed with an MRC1024 Bio-Rad confocal microscope (Bio-Rad Laboratories) with a 63×, 1.4 numerical aperture bright-field objective and the filter set at a $\lambda_{excitation}$ of 647 nm and a $\lambda_{emission}$ of 680 nm. Bandpass emission filters were used for the green and red channels and a longpass filter for the far red channel. Fluorescent dyes were imaged sequentially to eliminate cross talk between the channels. Images were merged and aligned using Adobe Photoshop 7.0 (Adobe Systems, Mountain View, CA), and fluorescence quantification was carried out using ImageJ software.

^{125}I-Tfn uptake and recycling. Holo-human Tfn was iodinated (1×10^6 to 2×10^6 cpm/μg) using chloramine T (Sigma Chemical Co.). TRVb-1 cell monolayers in 35-mm dishes (5×10^5 cells/dish) were infected with recombinant Sindbis viruses (2JC1, 2JC1-GFP-cRab22aWT, or 2JC1-GFP-cRab22aQ64L) at a multiplicity of infection of 50 PFU/cell in 200 μl PBS containing 1% FBS. Virus absorption was conducted at 4°C for 1 h. The infection mixtures were then replaced by 3 ml of Ham's F-12 medium containing 3% FBS, and the cells were incubated in a 37°C incubator for 8 h. After three washes with PBS at room temperature, the cells were incubated for 60 min at 37°C in internalization medium to deplete endogenous Tfn. For continuous uptake, the cells were incubated at 37°C for 30 min in internalization medium containing 6 μg/ml ^{125}I-Tfn. For surface binding, the cells were incubated with 6 μg/ml ^{125}I-Tfn in internalization medium for 90 min on ice. After Tfn internalization or surface binding, the cells were washed extensively in ice-cold 0.5% BSA and PBS, and the probe was chased at 37°C for different time periods in the presence of a 100-fold excess of unlabeled iron-saturated human Tfn and 100 μM deferoxamine mesylate. At each chase time, the medium was collected and the radioactivity was analyzed in a γ-counter to measure the amount of recycled Tfn. Cell surface-bound ^{125}I-Tfn was stripped by washing the cells three times alternately in ice-cold 0.1% BSA and PBS and in 0.1% BSA, 25 mM glacial acetic acid, and PBS (pH 4.2). The acid washes were pooled and counted. Approximately 90 to 95% of the surface-bound ^{125}I-Tfn was removed by the acid wash. To measure intracellular ^{125}I-Tfn, the cells were lysed in 1% Triton X-100 (Sigma Chemical Co.). Total cell-associated ^{125}I-Tfn was determined by adding surface-bound, recycled, and intracellular radioactivity. Nonspecific binding of ^{125}I-Tfn was determined by incubating the cells in internalization medium containing 6 μg/ml ^{125}I-Tfn and a 100-fold excess of unlabeled human Tfn for 90 min at 4°C. Cell surface-bound ^{125}I-Tfn was stripped by acid washes. These washes were pooled and counted. Nonspecific values were less than 10% of the specific binding.

Whole-cell lysates and Western blot analysis. TRVb-1 cell monolayers in 35-mm dishes (5×10^5 cells/dish) were infected with recombinant Sindbis viruses as described above. After 8 h of infection, cell monolayers were washed with ice-cold PBS and lysed in ice-cold lysis buffer (1% Nonidet P-40, 10% glycerol, 50 mM HEPES, 100 mM NaCl [pH 7.2]) containing a protease inhibitor cocktail (Sigma Chemical Co.). The lysates were vortexed and clarified by centrifugation at 16,000 × *g* for 15 min at 4°C. Protein concentration in lysates was determined using the bicinchoninic acid protein assay (Pierce Biotechnology Inc., Rockford, IL). The supernatants containing the cytosolic fraction of proteins were separated on 12% sodium dodecyl sulfate-polyacrylamide gels (25 μg protein per lane) and transferred to nitrocellulose membranes (Schleicher & Schuell, Keene, NH). Nonspecific binding was blocked by incubation of the membranes with 5% nonfat milk, 0.5% Tween 20, and PBS for 1 h at 37°C. The primary and secondary antibodies were diluted in blocking buffer and incubated overnight at 4°C and 1 h at room temperature. After each incubation step, the blots were washed five times for 7 min with 0.5% Tween 20 and PBS. Bound primary antibodies were visualized using peroxidase-conjugated secondary antibodies and an ECL detection system (Amersham Pharmacia Biotech, Piscataway, NJ).

Modeling of Tfn transport. Differential equations for Tfn transport in a two-endosomal compartment model have been described previously (see reference 21 and the supplemental material therein). Data were fitted to the model by minimization of $\Sigma[(\text{predicted values} - \text{observed values})^2]$. Rate constants were iteratively adjusted during the minimization process. These constants were defined as described previously (21). Statistical comparison of fits was performed by Fisher's F test as described in reference 14.

RESULTS

In CHO cells, the TfnR is trapped in Rab22a-containing vesicles. Three major routes are followed by proteins and lipids exiting sorting endosomes. Some macromolecules are directed to lysosomes, others are directed to the TGN, and another set is recycled back to the cell surface. We have observed that expression of GFP-cRab22a in CHO cells causes a striking enlargement of the sorting endosomes (13). In these cells, transport to lysosomes is not disrupted. In contrast, a remarkable delay in transport from endosomes to the TGN was observed (12). We wondered whether cRab22a expression affects the recycling of macromolecules to the cell surface, the other major route. Specifically, we were interested in Tfn recycling that has been well characterized in TRVb-1 cells, a CHO cell line stably expressing the human TfnR.

According to published results, in TRVb-1 cells, TfnRs localize predominantly in the recycling center, and a minor percentage is present in early endosomes scattered throughout the cell. This pattern of distribution was observed in untransfected cells (Fig. 1B and E) or cells expressing GFP alone (Fig. 1B). However, the distribution of the receptor was strikingly different in cells expressing cRab22aWT or the Q64L mutant. In these cells, most of the TfnR localized in large cRab22a-containing endosomes in the periphery of the cell (Fig. 1E and H). These observations indicate that in CHO cells, expression of cRab22a alters the distribution of TfnR that is trapped in large cRab22a-containing vesicles.

Rab22a affects the intracellular distribution of other proteins involved in recycling. The TfnR traverses a complex intracellular route to transport Tfn in and out of the cell. We wondered whether other molecules that participate in TfnR transport are affected by cRab22a overexpression in CHO cells. For these experiments, cRab22aWT was subcloned in the

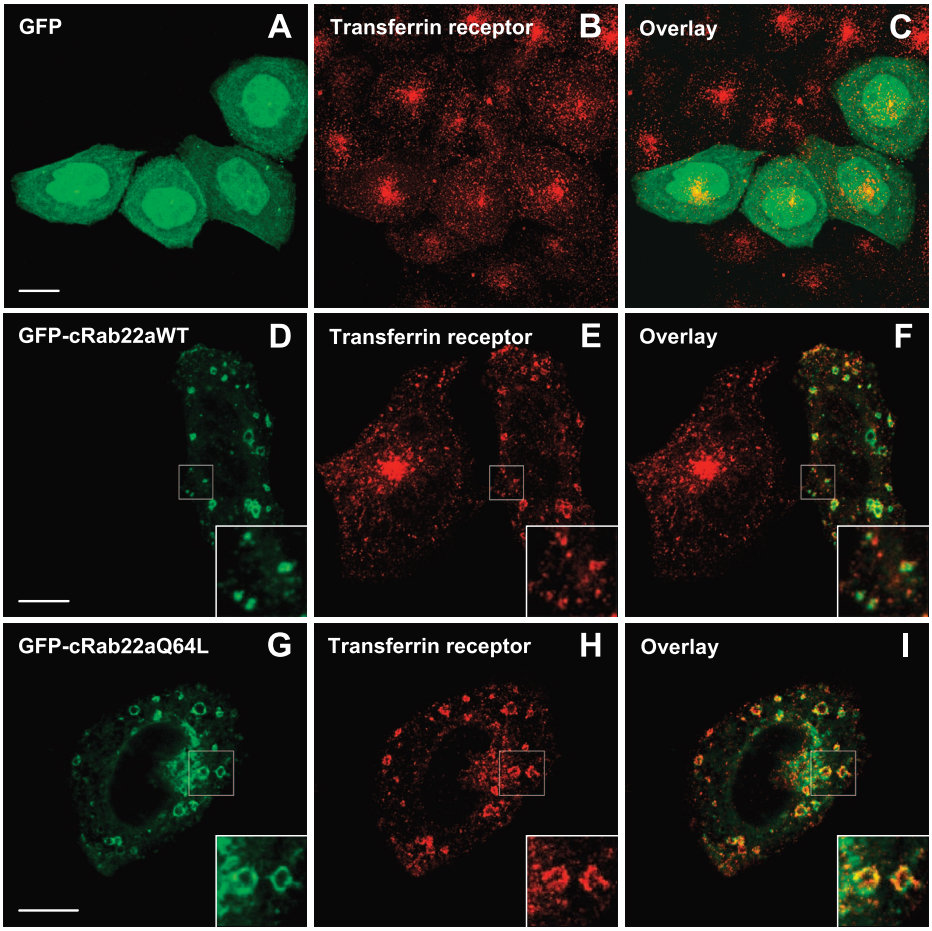

FIG. 1. Expression of Rab22aWT or Rab22aQ64L redistributes the TfnR in CHO cells. TRVb-1 cells were transiently transfected with pEGFP-C1 (A to C), pEGFP-C1-cRab22aWT (D to F), or pEGFP-C1-cRab22aQ64L (G to I). Eighteen hours later, the cells were fixed and labeled with a monoclonal anti-human TfnR antibody and analyzed in a confocal microscope. Images (summation of all confocal planes) were merged and aligned using Adobe Photoshop 7.0. Bars, 10 μm.

pERFP vector and coexpressed with other proteins cloned in different pEGFP vectors. RFP-cRab22aWT has an intracellular localization identical to that of GFP-cRab22aWT (when coexpressed in the same cells, they show virtually complete colocalization) (data not shown). hRab5a (Fig. 2A to C) and hRab4a (Fig. 2E to G) were found in cRab22a-containing vesicles. Also, cRab22a presented a very prominent colocalization with human cellubrevin, an R-SNARE that participates in the recycling of the TfnR to the cell surface (Fig. 2I to K). It is interesting to observe that the distribution pattern of these three proteins was altered by cRab22a overexpression. When expressed alone, hRab5a was present in small scattered vesicles (Fig. 2D). Coexpression with cRab22a caused a significant increase in the size of the hRab5a-containing vesicles (compare insets in Fig. 2A to D). hRab4a and human cellubrevin localized preferentially to the perinuclear region when expressed alone (Fig. 2H and L). Expression of cRab22a redistributes most of hRab4a (Fig. 2E to G) and human cellubrevin (Fig. 2I to K) to peripheral large vesicles containing cRab22a. The effect on hRab11a was less prominent. This small GTPase remained in a large percentage in a perinuclear region, which is its normal localization (Fig. 2M to O). However, the amount of hRab11a-positive vesicles in the periphery increased in cells expressing cRab22a. Most of these vesicles also contained cRab22a. It is worth mentioning that these effects were observed at all levels of expression. However, more dramatic redistributions of hRab4a, human cellubrevin, and hRab11a were observed in cells with a high content of cRab22a. Figure 2 shows cells with medium levels of expression. Colocalization was high even in cells where cRab22a-associated fluorescence was low (86%, 88%, 74%, and 69% of cRab22a-positive vesicles contained hRab5a, hRab4a, human cellubrevin, and hRab11a, respectively) (see Fig. S1 in the supplemental material).

Overexpression of Rab22a prevents recycling of Tfn in CHO cells. We observed that expression of cRab22a in CHO cells causes a striking redistribution of TfnR from the pericentriolar region to large cRab22a-containing vesicles. To assess whether this alteration in receptor distribution affected Tfn recycling, cells transfected with pEGFP-C1, pEGFP-C1-cRab22aWT, or pEGFP-C1-cRab22aQ64L were incubated for 30 min at 37°C with tetramethylrhodamine-labeled Tfn to load all intracellular compartments. The cells were then washed and incubated in medium with an excess of unlabeled Tfn to follow the recycling of this protein to the medium.

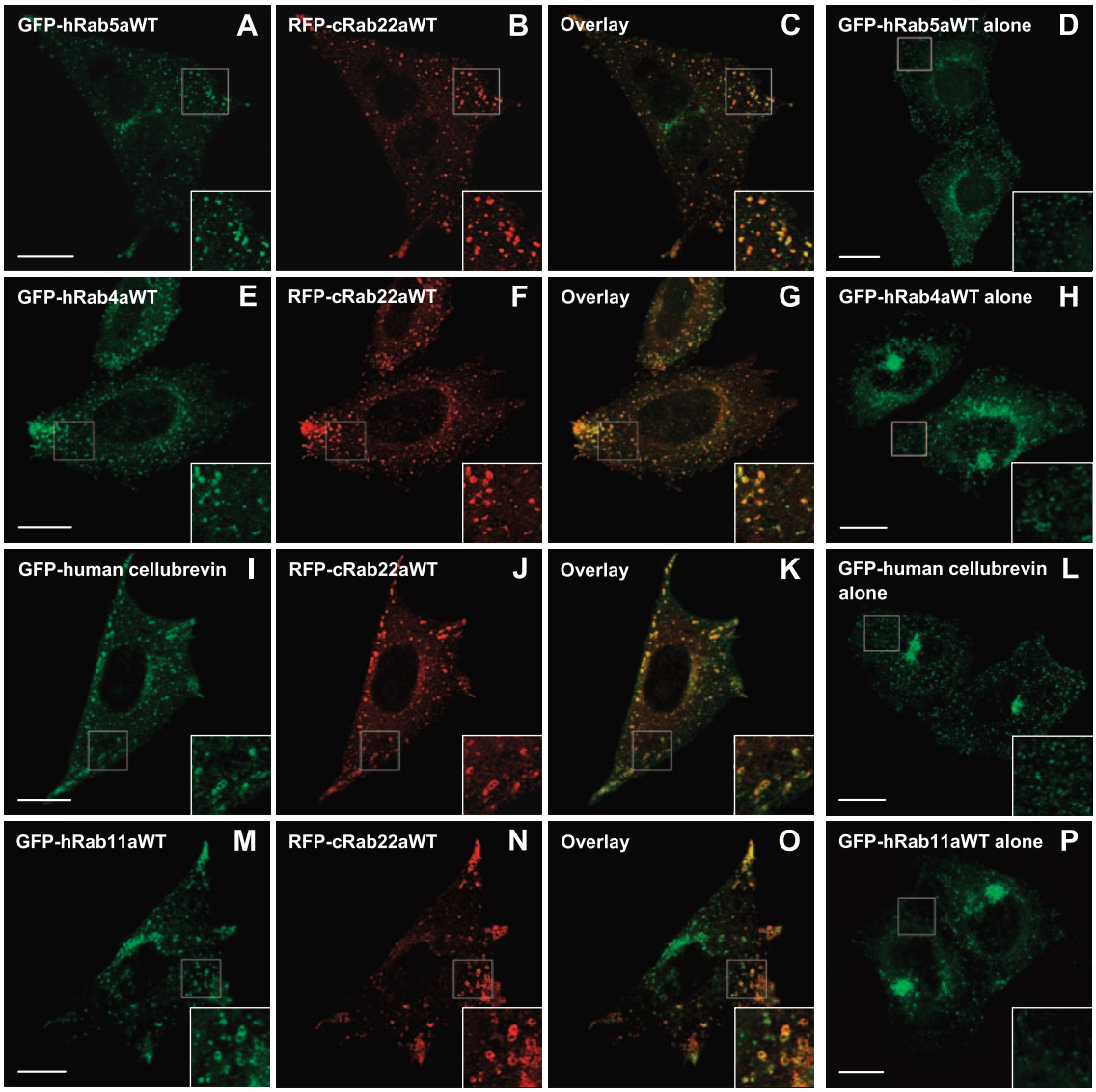

FIG. 2. Several proteins that participate in Tfn recycling are redistributed by expressing Rab22a. TRVb-1 cells were cotransfected with pERFP-cRab22aWT and pEGFP-C1-hRab5aWT (A to C), pCMV-EGFP-C3-hRab4aWT (E to G), pEGFP-C3-human cellubrevin (I to K), or pEGFP-C1-hRab11aWT (M to O). Eighteen hours later, cells were fixed and the distribution of the fluorescent proteins was recorded in a confocal microscope. As a control, cells transfected with the same pEGFP constructs alone are shown in the right panels (D, H, L, and P). To facilitate comparisons, the same magnification is shown in insets for single- and double-transfected cells. Images (single confocal plane) were merged and aligned using Adobe Photoshop 7.0. Bars, 10 μm.

After a 30-min uptake, untransfected and transfected cells presented intense Tfn labeling. However, in untransfected cells or cells expressing GFP alone, Tfn accumulated in the recycling center and in small vesicles throughout the cytoplasm (Fig. 3B and E). In contrast, in cells expressing cRab22aWT or cRab22aQ64L (data not shown), Tfn localized in large cRab22a-containing endosomes in the periphery of the cell (Fig. 3E). With subsequent incubations, Tfn rapidly disappeared from untransfected cells (data not shown) and from GFP-expressing cells (Fig. 3H). However, cells expressing cRab22aWT (Fig. 3K) or the Q64L mutant (data not shown) retained Tfn for more than 1 hour. Quantification of the morphological data showed that during the first few minutes, all cells recycled Tfn at the same rate (Fig. 3M). However, after a 1-hour chase, about 50% of the internalized Tfn was still present in cells expressing cRab22a (wild type or Q64L mutant), whereas the label was barely detectable in cells expressing GFP (Fig. 3M). Note that 70% to 80% of cRab22a-positive vesicles retained Tfn throughout the chase period (Fig. 3N).

To further confirm the effects of cRab22a expression, recycling was measured biochemically using radiolabeled Tfn. Cells were treated with Sindbis viruses containing cRab22a (wild type and Q64L mutant) to obtain high percentages of cRab22a-expressing cells. The levels of expression were similar in both cell lines as estimated by Western blotting (Fig. 4A). The amount of endogenous Rab22a was about one-fifth of that of the recombinant canine protein (Fig. 4A). The recycling results shown in Fig. 4B and C are qualitatively and quantitatively similar to

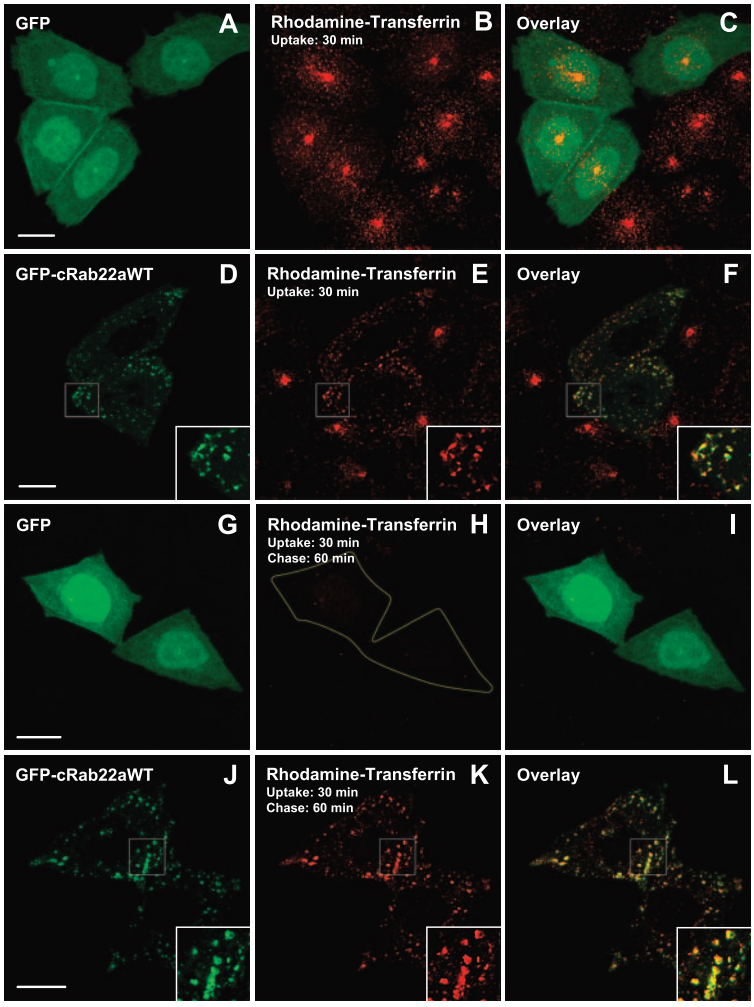

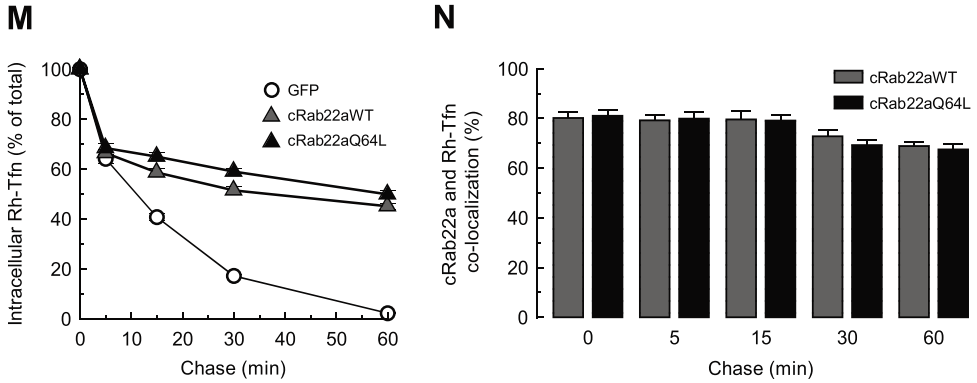

FIG. 3. Expression of Rab22a inhibits the recycling of fluorescent Tfn. TRVb-1 cells transfected with pEGFP-C1, pEGFP-C1-cRab22aWT, or pEGFP-C1-cRab22aQ64L were incubated for 30 min at 37°C with tetramethylrhodamine-labeled Tfn. The cells were then washed and incubated in prewarmed internalization medium containing an excess of unlabeled Tfn for 0, 5, 15, 30, or 60 min at 37°C. Cells were fixed, and the distribution of the fluorescent proteins was recorded in a confocal microscope. After a 30-min uptake, both untransfected and transfected cells presented intense Tfn labeling. However, in untransfected cells (B and E) or cells expressing GFP alone (B), Tfn accumulated in the recycling center and in small vesicles throughout the cytoplasm. In contrast, in cells expressing cRab22aWT, Tfn localized in large cRab22a-containing endosomes in the periphery of the cell (D to F). When the cells were chased for 60 min, Tfn disappeared from untransfected cells and GFP-expressing cells (H). However, cells expressing cRab22aWT retained Tfn in cRab22a-positive compartments (J to L). Images (summation of all confocal planes) were merged and aligned using Adobe Photoshop 7.0. Bars, 10 μm. Quantification of the morphological data for cells expressing GFP (white circles), GFP-cRab22aWT (gray triangles), or GFP-cRab22aQ64L (black triangles) is shown in panel M. Note that cRab22a-positive structures retain Tfn throughout the chase period in cells expressing GFP-cRab22a (wild type, gray bars; Q64L, black bars) (N). The data in panels M and N represent the means ± standard errors of the means from three independent experiments quantified as explained in Materials and Methods.

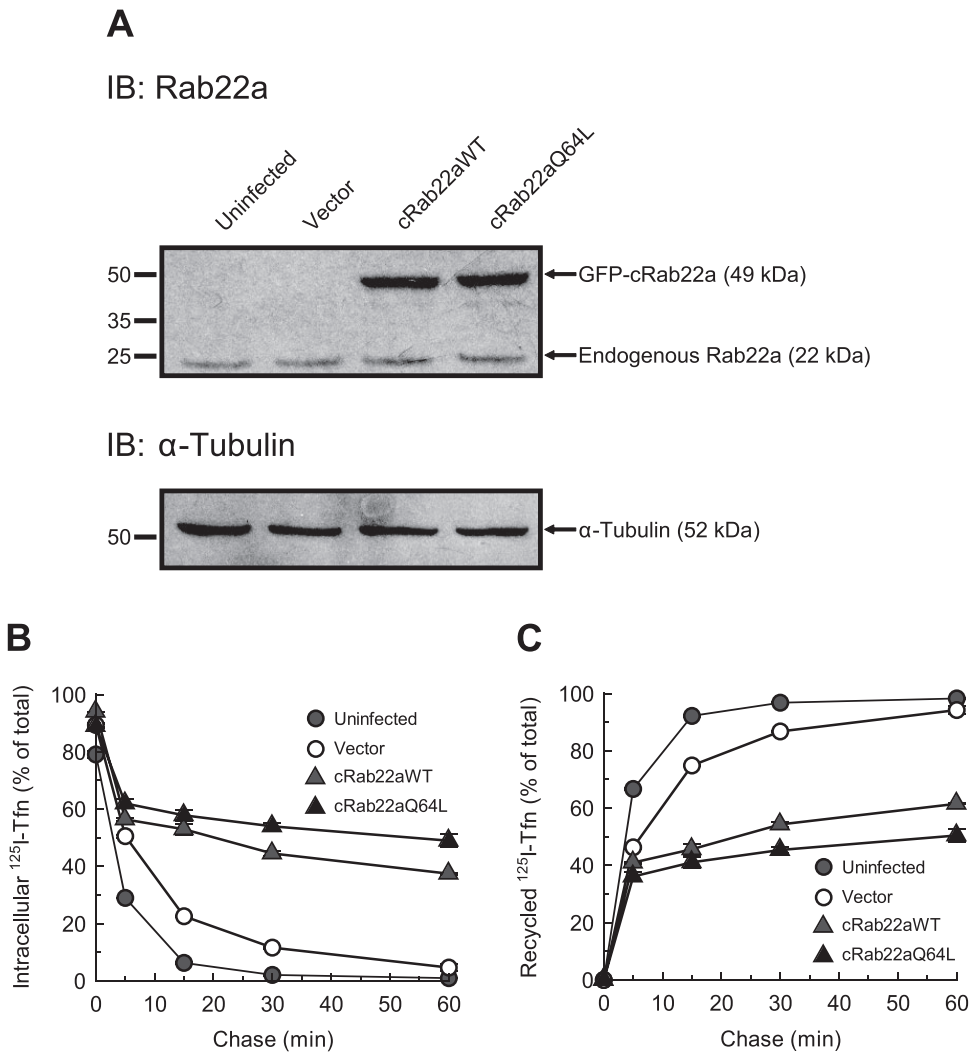

FIG. 4. Expression of Rab22a inhibits the recycling of ^{125}I-Tfn. (A) To assess cRab22a expression level, uninfected TRVb-1 cells (uninfected) or cells infected with 2JC1 (vector), 2JC1-GFP-cRab22aWT (cRab22aWT), or 2JC1-GFP-cRab22aQ64L (cRab22aQ64L) were solubilized and analyzed by Western blotting using a polyclonal anti-Rab22a-specific antibody (20 μg/ml) (top panel). To estimate loading, the samples were analyzed with a monoclonal anti-α-tubulin antibody (0.2 μg/ml) (bottom panel). (B and C) Uninfected TRVb-1 cells (gray circles) or cells infected with 2JC1 (white circles), 2JC1-GFP-cRab22aWT (gray triangles), or 2JC1-GFP-cRab22aQ64L (black triangles) were incubated with 6 μg/ml ^{125}I-Tfn for 30 min at 37°C. The cells were washed, and the probe was chased for different periods of time in the presence of an excess of unlabeled Tfn. At each chase period, the medium was collected and counted in a γ-counter to measure the amount of recycled Tfn. Cell surface-bound ^{125}I-Tfn was stripped by an acid-wash method and counted. Surface-associated Tfn represented less than 10% of the total radioactivity (data not shown). Intracellular Tfn was measured in cell lysates. (B) Intracellular Tfn at different chase periods. (C) Recycled Tfn at different chase periods. The data represent the means ± standard errors of the means from two independent experiments carried out in duplicate.

those obtained with fluorescent Tfn (Fig. 3M). The initial rates of recycling were similar for all cells (Fig. 4B and C). However, after a 30-min chase, most of the protein had recycled into the medium in untransfected cells or cells expressing GFP, whereas about 60% of the Tfn initially bound to the cells was retained in cells expressing cRab22aWT or cRab22aQ64L.

These observations indicate that cRab22aWT and the GTPase-deficient mutant retain Tfn in cRab22-positive vesicles and prevent the normal recycling of this molecule to the cell surface.

Rab22a expression causes retention of Tfn in a compartment with slow recycling kinetics. To assess the effect of cRab22a on a single wave of internalization, TRVb-1 cells expressing GFP, GFP-cRab22aWT, or GFP-cRab22aQ64L were incubated with tetramethylrhodamine-conjugated Tfn at 4°C. Afterward, the cells were washed and transferred to 37°C. At different time periods, cells were acid washed to eliminate surface-bound fluorescent Tfn and subsequently fixed. At 4°C, before the acid wash, Tfn was confined to the plasma membrane (Fig. 5B and E). Note that the labeling was less intense in cells expressing cRab22a proteins. After a very short period of chase at 37°C (≅2 min), Tfn was found in small vesicles lacking cRab22a (data not shown). A few minutes later (≅5 min), Tfn localized in cRab22a-positive compartments (data not shown). With longer incubation periods, Tfn disappeared from untransfected cells whereas it was retained in transfected cells in cRab22a-positive endosomes (Fig. 5H and K). A cell-

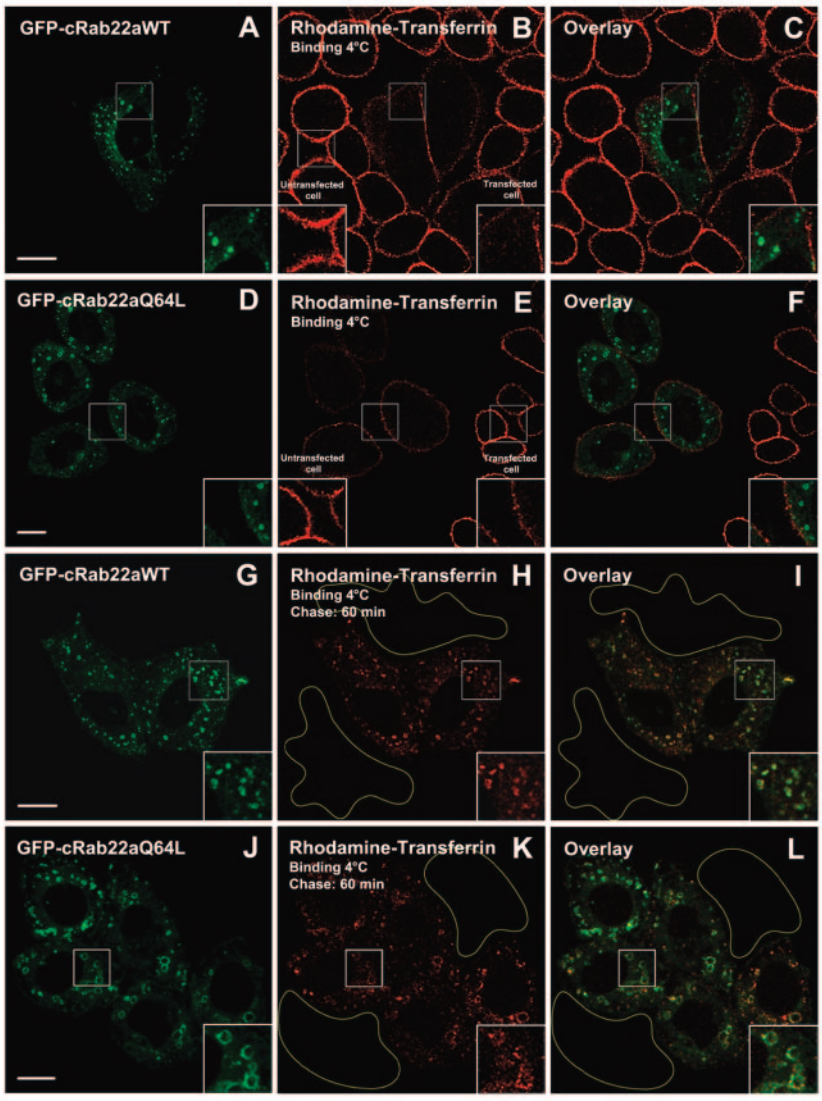

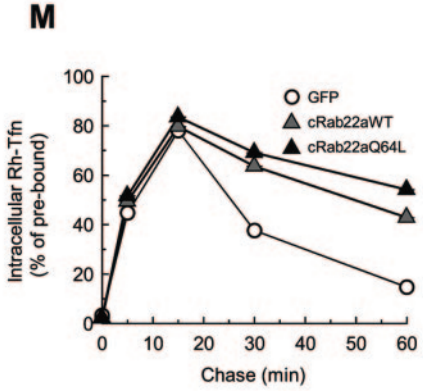

FIG. 5. The rate of Tfn internalization is not affected by Rab22a, but recycling is impaired. TRVb-1 cells transfected with pEGFP-C1-cRab22aWT or pEGFP-C1-cRab22aQ64L were incubated for 90 min at 4°C with tetramethylrhodamine-labeled Tfn. The cells were then washed and incubated in medium containing an excess of unlabeled Tfn for 0, 5, 15, 30, or 60 min at 37°C. Surface-bound fluorescent Tfn was removed by the acid-wash method (except at 0 min). Cells were fixed, and the distribution of the fluorescent proteins was recorded in a confocal microscope. After the binding period at 4°C, all Tfn was present in the cell surface, both in untransfected cells (B and E) and cells expressing cRab22aWT (B) or cRab22aQ64L (E). Note that surface binding was lower in transfected cells (B and E). Despite the low initial binding, Tfn was present only in cells expressing cRab22aWT (G to I) or the Q64L mutant (J to L) after a 60-min chase period. In these cells, Tfn was retained in cRab22a-positive structures. Images (summation of all confocal planes) were merged and aligned using Adobe Photoshop 7.0. Bars, 10 μm. Quantification of the morphological data from three experiments for cells expressing GFP (white circles), GFP-cRab22aWT (gray triangles), or GFP-cRab22aQ64L (black triangles) is shown in panel M (means ± standard errors of the means).

associated fluorescence quantification of the images is shown in Fig. 5M. At early time points, no significant differences were observed, suggesting that the internalization rate was unaffected by expression of cRab22a. In contrast, at late time points, a significant amount of the initially bound Tfn (about 50%) was found only in cRab22a-expressing cells. Sindbis virus-infected cells were used to carry out the same kinds of experiments with radiolabeled Tfn. The results in Fig. 6A to C show that Tfn is normally internalized from the cell surface in cells expressing cRab22a but that recycling to the medium is delayed. A prediction from this conclusion is that the amount of TfnR on the cell surface should decrease in these cells. This prediction is consistent with the reduced Tfn binding at 4°C observed in Fig. 5A to F. Fluorescence quantification of these images showed a 60% reduction of the surface labeling (Fig. 7A). Quantification of the cell-associated ^{125}I-labeled Tfn after binding at 4°C in virus-infected cells showed a similar reduction of Tfn receptors on the cell surface (Fig. 7B).

The kinetics of recycling in CHO cells have been modeled by assuming the existence of two compartments (E1 and E2, which correspond to early and recycling endosomes, respectively, in untreated cells) from which Tfn can be transported back to the medium (Fig. 6D) (21). By using the same equations describing the transit of the ligand between compartments, we have optimized the rate constants to fit our experimental data obtained in uninfected cells and cells infected with control Sindbis viruses (Fig. 6F). The values of the constants for these cells are listed in Table 1. Differences in the published values were minor and may be attributed to the fact that CHO cytoplasts instead of entire cells were used (21). In contrast, in cells expressing cRab22aWT or the Q64L mutant (similar results were obtained for both proteins, and the fitting was performed by combining both sets of data) (Fig. 6G), some rate constants changed dramatically whereas others were not affected. Arrival to and recycling from the early compartment (E1) were not significantly changed (Table 1). In contrast, there was almost no recycling from E2 to the plasma membrane ($k_3 \cong 0$), and the kinetics of return from E2 to E1 was also very slow (Table 1 and Fig. 6E). Therefore, in cRab22a-expressing cells, the properties of the second intracellular compartment E2 were completely different from those of recycling endosomes. This indicates that expression of cRab22a forces Tfn into a compartment that behaves as a sink from which recycling is very slow.

Tfn is retained in early compartments of the endocytic pathway. The kinetic analysis indicates that in CHO cells expressing cRab22aWT or cRab22aQ64L, Tfn is delivered to a special intracellular compartment with low recycling rate constants. On the other hand, the morphological observations indicate that Tfn is retained in a cRab22a-positive compartment (Fig. 3 and 5). According to previous results, most cRab22a-labeled structures are accessible to molecules internalized by fluid phase and receptor-mediated endocytosis after a short period of uptake (≅5 min), indicating that these structures are early/sorting endosomes (9, 12, 13). To confirm the nature of the compartments in which Tfn was retained, we performed triple staining experiments with some specific markers. For these experiments, intracellular Alexa Fluor 647-conjugated Tfn was allowed to reach a steady state by a 30-min uptake at 37°C, followed by a 60-min chase in the continuous presence of an excess of unlabeled Tfn. After fixation, the cells were immunolabeled with different antibodies or incubated with the acidotropic dye LysoTracker Red DND-99. The results indicate that most Tfn-containing compartments were positive for EEA1 and cRab22a, indicating that Tfn was retained in early/sorting endosomes (Fig. 8A to D). In contrast, very little colocalization with LBPA (Fig. 8E to H), cathepsin D (Fig. 8I to L), or LysoTracker Red (Fig. 8M to P) was observed, indicating that Tfn was not mistargeted to late endosomes or lysosomes. Similar results were obtained with the cRab22aQ64L mutant, although some colocalization between Tfn and cathepsin D in cRab22a-positive vesicles was observed in these cells (data not shown). These observations indicate that in cells expressing cRab22aWT or the Q64L mutant, Tfn is retained mostly in early compartments of the endocytic pathway.

Tfn is retained in a compartment that is not affected by brefeldin A. The large cRab22a-containing compartments are likely early/sorting endosomes. Another possibility is that they are deformed recycling endosomes that have lost their perinuclear localization. BfA promotes mixing and tubulation of several membrane-bound structures. In particular, recycling endosomes form a prominent tubulated, perinuclear compartment (22). To assess whether Tfn was retained in a recycling compartment sensitive to BfA, cells expressing GFP alone, GFP-cRab22aWT, or GFP-cRab22aQ64L (data not shown) were loaded with fluorescent Tfn in the continuous presence of BfA. In untransfected cells or in cells transfected with pEGFP-C1, BfA caused the appearance of Tfn-loaded tubules in the pericentriolar region (Fig. 9B and untransfected cells in Fig. 9E). However, in cells expressing cRab22aWT or the Q64L mutant (data not shown), Tfn/cRab22a-containing compartments did not tubulate (Fig. 9E). Tubules were also evident in BfA-treated cells expressing hRab4aWT, human cellubrevin, or hRab11aWT (Fig. 9J, N, and R). However, in cells coexpressing RFP-cRab22aWT and GFP-hRab4aWT (Fig. 9G to I) or GFP-human cellubrevin (Fig. 9K to M), Tfn was found in compartments containing both overexpressed proteins that did not tubulate with BfA. When cRab22aWT and hRab11aWT were coexpressed, the perinuclear structures containing hRab11a and Tfn but not cRab22a were found to be tubulated. In contrast, compartments in the periphery containing hRab11a, cRab22a, and Tfn remained as round structures (Fig. 9O to Q). Moreover, cRab22a appears to have a phenotype dominant over those of hRab4a and human cellubrevin, since the distribution of Tfn in cotransfected cells resembled that observed in cells expressing cRab22a alone. From these experiments, we conclude that overexpression of cRab22a causes the retention of Tfn in enlarged endosomes that are not affected by BfA. These structures are enriched in several proteins that participate in recycling and sorting, suggesting that they are modified sorting endosomes.

Rab22a expression affects Tfn intracellular transport in HeLa cells. In a recent paper, it was shown that overexpression of cRab22a in HeLa cells affects the recycling of MHC-I molecules from endosomes to the plasma membrane whereas the recycling of Tfn is not altered (28). Reports from this and other laboratories have shown that the phenotype of HeLa cells expressing cRab22a is very different from that observed in CHO cells (9, 28). To analyze the effect of our constructs on Tfn recycling in HeLa, this cell line was transfected with pEGFP-C1,

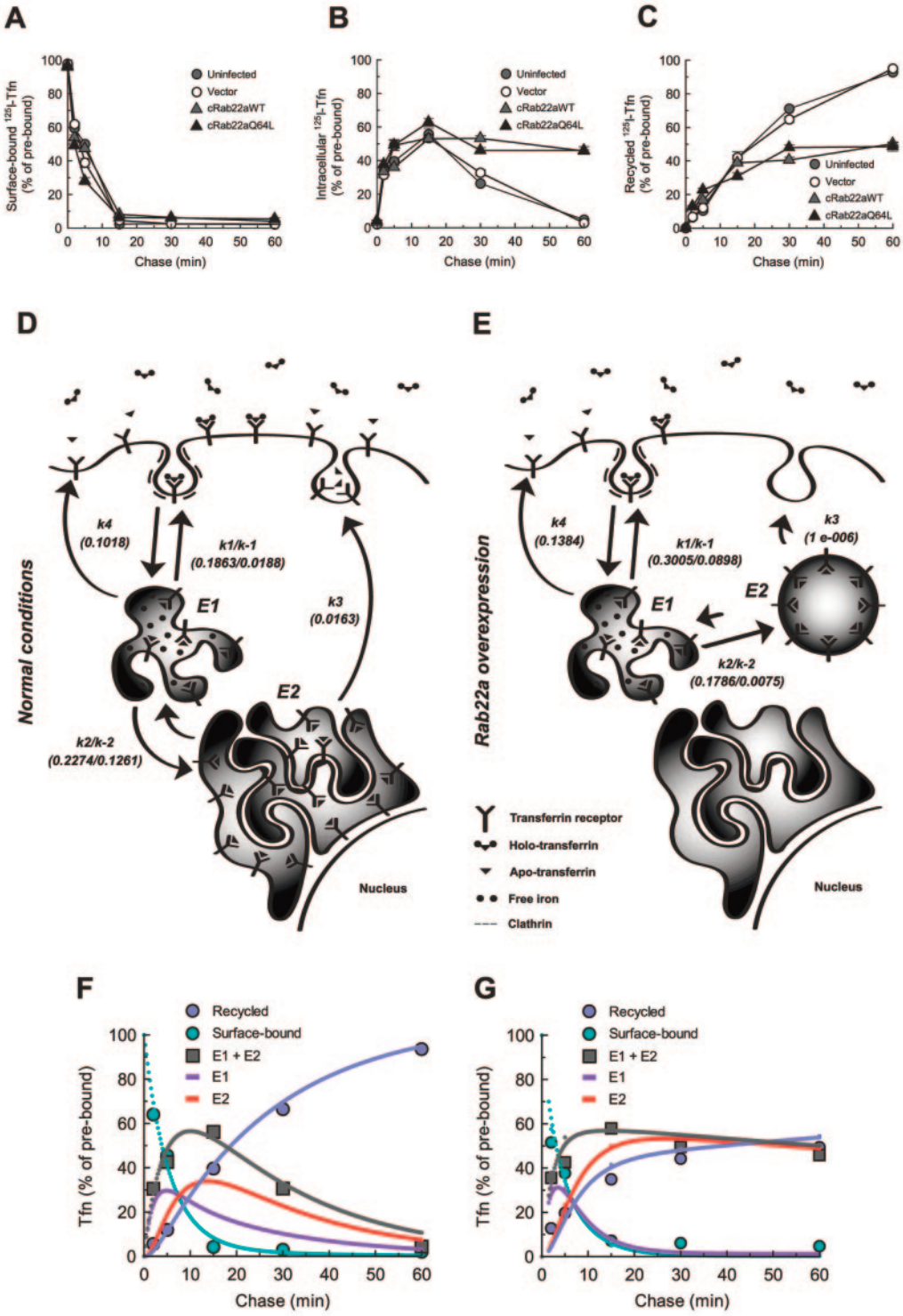

FIG. 6. Rab22a expression retains Tfn in a compartment with slow recycling kinetics. Uninfected TRVb-1 cells (gray circles) or cells infected with 2JC1 (white circles), 2JC1-GFP-cRab22aWT (gray triangles), or 2JC1-GFP-cRab22aQ64L (black triangles) were incubated with 6 μg/ml ^{125}I-Tfn for 90 min at 4°C. The cells were washed, and the probe was chased for different periods of time in the presence of an excess of unlabeled Tfn. At each chase time period indicated, the medium was collected and counted to measure recycled Tfn. Cell surface-bound ^{125}I-Tfn was stripped by an acid-wash method and counted. Intracellular Tfn was measured in cell lysates. The results for surface-bound (A), intracellular (B), and recycled (C) ^{125}I-Tfn from two independent experiments carried out in duplicate are shown at different chase periods. Data in panels A to C from uninfected cells and cells infected with control Sindbis viruses were combined and adjusted to a kinetic model depicted in panel D. Experimental and predicted values are shown in panel F. Data in panels A to C from cells overexpressing cRab22a (wild type or Q64L mutant) were combined and adjusted to a kinetic model depicted in panel E (see text). Experimental and predicted values are shown in panel G. For panels F and G, large scattered symbols correspond to experimental data, and small continuous symbols correspond to predicted values. Percentages of Tfn that are cell surface bound (turquoise), recycled to the medium (light blue), and intracellular (E1 and E2) (gray) and the predicted values for E1 (violet) and E2 (red) are shown.

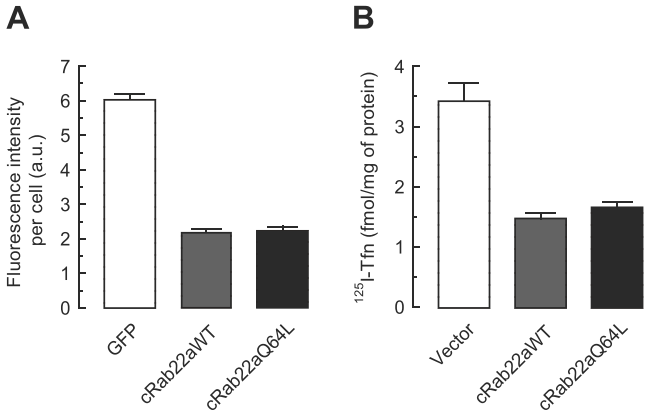

FIG. 7. Rab22a expression diminishes TfnR on the cell surface. (A) Cell surface fluorescence in cells treated as described in the legend to Fig. 5 (i.e., 4°C Tfn binding without chase) was quantified in transiently transfected cells with pEGFP-C1 vector (white bar) and cells expressing GFP-cRab22aWT (gray bar) or GFP-cRab22aQ64L (black bar). The results are expressed in arbitrary units per cell. (B) Cell surface-bound ^{125}I-Tfn was measured in cells treated as explained in the legend to Fig. 6 (i.e., 4°C Tfn binding without chase) infected with 2JC1 (white bar), 2JC1-GFP-cRab22aWT (gray bar), or 2JC1-GFP-cRab22aQ64L mutant (black bar) and normalized for protein content. Values represent the means ± standard errors of the means from three (A) or two (in duplicate) (B) independent experiments.

pEGFP-C1-cRab22aWT, or pEGFP-C1-cRab22aQ64L and immunostained with a monoclonal anti-human TfnR antibody. In most cells, the cRab22a wild type and the Q64L mutant were found in small vesicles in the perinuclear region and in the cell periphery (Fig. 10E and H). These vesicles only seldom contained TfnR labeling (Fig. 10E to J), very different from the images shown in Fig. 1 for TRVb-1 cells. Also, note that the distribution of TfnR was not significantly altered in HeLa cells expressing cRab22aWT or cRab22aQ64L proteins (Fig. 10F and I).

Most of the studies carried out with Rab22a overexpression have used the canine protein. Human and canine Rab22a have a perfect match except for three amino acids in the carboxy-terminal domain (Fig. 10A). We wondered whether the lack of effect of cRab22a in TfnR distribution could be due to the fact that some Rab22a-interacting proteins in HeLa cells do not recognize the canine protein. Rab6A and Rab6A′ differ in only three amino acids, and yet, they have different functions in the retrograde transport (6). Consequentially, we decided to clone hRab22a in pEGFP-C1 vector and to generate the Q64L mutant. When these proteins were expressed in HeLa cells, hRab22aWT and hRab22aQ64L were found in large round-shaped vesicles (Fig. 10K and N). Colocalization with the TfnR was prominent especially for the Q64L mutant (Fig. 10K to P). hRab22a was also found in long tubular structures lacking TfnR (left insets in Fig. 10N to P). To test whether hRab22a could affect the recycling of Tfn in the HeLa cell line, the cells were allowed to internalize tetramethylrhodamine-conjugated Tfn for 30 min and were then incubated for different periods of time at 37°C in the presence of an excess of unlabeled protein. Under these conditions, cells expressing hRab22aWT (data not shown) and hRab22aQ64L (Fig. 11A to L) retained Tfn in hRab22a-positive structures. Quantification of the morphological data showed that initially, all cells recycled Tfn with the same kinetics. Afterward, about 50% of the internalized Tfn was retained in cells expressing hRab22a (wild type or Q64L mutant) whereas it disappeared from cells expressing GFP (Fig. 11M). The effect was very similar to that observed with cRab22a in TRVb-1 cells (compare Fig. 3M and 11M). In HeLa cells, 70% to 80% of hRab22a-positive vesicles retained Tfn throughout the chase period (Fig. 11N).

In conclusion, expression of Rab22a also affects Tfn transport in HeLa cells. For some still-unknown reason, this cell line seems to be able to distinguish between canine and human Rab22a, with the canine isoform causing only a minor effect on Tfn transport. In contrast, the human protein strongly affects TfnR distribution and Tfn recycling. To assess whether this was a cell-specific effect, several cell lines were transfected with human and canine Rab22aQ64L and were allowed to internalize fluorescent Tfn for 30 min at 37°C. The human protein caused the formation of large ring-shaped structures loaded with Tfn in all cells. The phenotype was stronger for hRab22aQ64L than for cRab22aQ64L in HEK 293 (human) and Vero (African green monkey) cells, suggesting that other cell lines can also distinguish between the two proteins. In contrast, both proteins have the same strong effect on TRVb-1 (Chinese hamster) and BHK-21 (Syrian golden hamster) cells (see Fig. S2 in the supplemental material).

Endogenous Rab22a associates with compartments containing internalized Tfn. Expression of the Rab22a wild type and the GTPase-deficient mutant strongly affects the morphology of endosomes. Moreover, it inhibits Tfn recycling and promotes the redistribution of TfnR to large Rab22a-containing vesicles. Therefore, the distribution of these recombinant proteins may not reflect the normal localization of endogenous Rab22a. To assess the localization of this protein, an anti-Rab22a-specific antibody was optimized for immunofluorescence assays. Note that the peptide used for raising the antibody is common for cRab22a and hRab22a. Under the conditions used, the labeling in CHO and HeLa cells was completely blocked by preincubation with the Rab22a peptide (see Fig. S3 in the supplemental material). In CHO cells, endogenous Rab22a was found in small vesicles and in short tubules (Fig. 12A to C) (see Fig. S3 in the supplemental material). Colocalization with Tfn was observed principally in vesicular structures

TABLE 1. Rate constants for Tfn trafficking in control and Rab22a-expressing cells[a]

Variable	Rate constant (min^{-1}) for Tfn trafficking	
	Control	cRab22a overexpression
k_1	0.1863	0.3005*
k_{-1}	0.0188	0.0898^{NS}
k_2	0.2274	0.1786^{NS}
k_{-2}	0.2274	0.0075**
k_3	0.1201	1.00×10^{-6}**
k_4	0.1018	0.1384^{NS}

[a] The rate constants (k) adjusted to the experimental data shown in Fig. 6F (control column) and in Fig. 6G (cRab22a overexpression column) are shown. Comparisons among rate constants in control and cRab22a-expressing cells are shown in the right column (*, $P < 0.01$; **, $P < 0.0001$; NS, $P > 0.05$). To assess whether a rate constant was significantly affected by cRab22a expression, the value obtained in uninfected cells (control column) was maintained fixed, and the other five rate constants were adjusted to fit the data in cRab22a-expressing cells (Fig. 6G). The final sum of squares was compared with the sum of squares obtained when the six constants were freely adjusted (14).

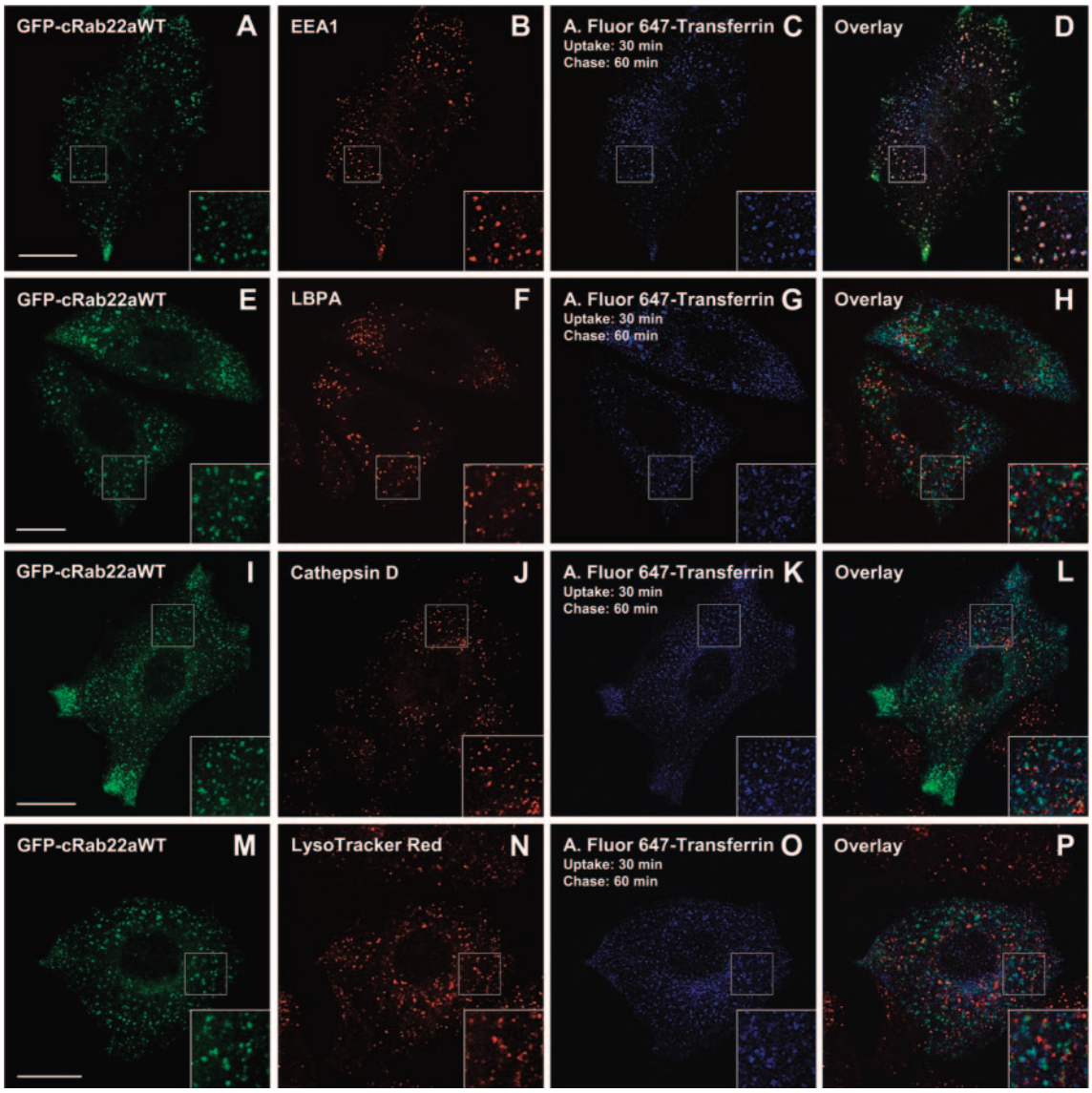

FIG. 8. Tfn is retained in early endocytic compartments in Rab22a-expressing cells. TRVb-1 cells expressing GFP-cRab22aWT (green channel) were labeled with Alexa Fluor 647-conjugated Tfn (blue channel) for a 30-min uptake at 37°C, followed by a 60-min chase period. Cells were fixed and immunostained (red channel) with antibodies recognizing EEA1 (A to D), LBPA (E to H), or cathepsin D (I to L). Acidic compartments were labeled with LysoTracker Red DND-99 (M to P). Images (single confocal plane) were merged and aligned using Adobe Photoshop 7.0. Bars, 10 μm.

(Fig. 12A to C). In HeLa cells, Rab22a was also observed in small vesicles and, as previously described (28), in prominent long tubules that did not contain Tfn (Fig. 12G to I) (see Fig. S3 in the supplemental material). Note that very little Rab22a was present in the perinuclear recycling center (Fig. 12A to C and G to I) and that upon BfA treatment, Rab22a distribution was not affected (Fig. 12D to F and J to L). In the treated cells, Tfn localized with Rab22a in round vesicles but not in the tubular structures induced by the drug. All these results suggest that Rab22a is not present in perinuclear recycling endosomes. To better define the compartments within the Tfn pathway that contain endogenous Rab22a, TRVb-1 cells were incubated at 4°C with the protein and then warmed up to 37°C for different periods of time. Very scarce colocalization was observed at 0, 1, and 2 min of chase (data not shown). The amount of vesicles containing both Rab22a and Tfn was maximal after 5 to 8 min (cells after an 8-min chase are shown in Fig. 12M to O). After 16 min, a large percentage of Tfn was found in a perinuclear localization with low colocalization with Rab22a (data not shown), suggesting that the endogenous GTPase is present in compartments upstream of the recycling endosomes. The same protocol could not be used with HeLa cells because the fluorescence signal after the 4°C binding was low. However, consistent with a distribution in early/sorting endosomes, improved Rab22a colocalization with Tfn was observed when the transport to the perinuclear endosomes was delayed by performing the uptake at 16°C (Fig. 12P to R). In conclusion, our results indicate that Tfn enters in Rab22a-containing vesicles before being transported to the perinuclear recycling center.

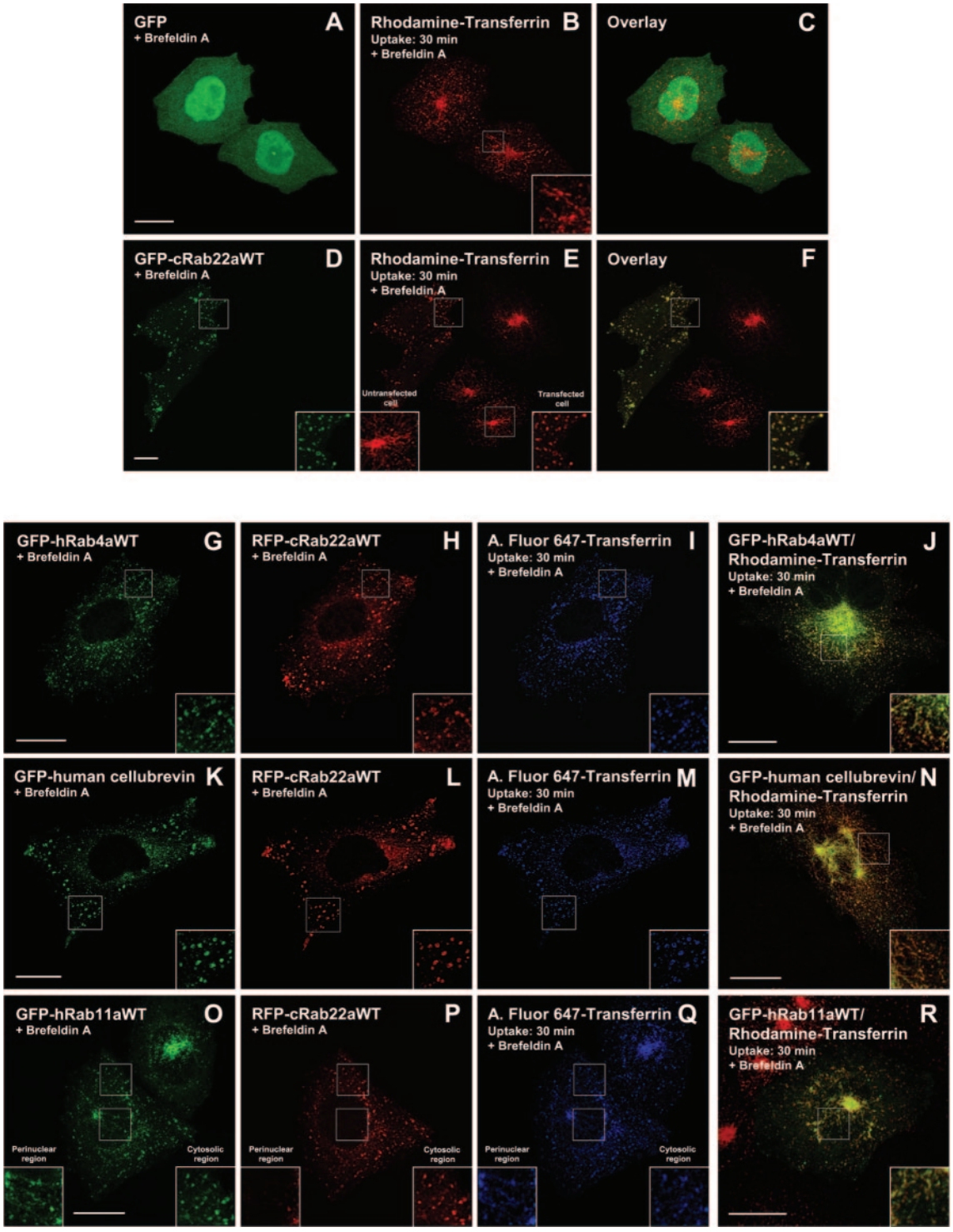

FIG. 9. Tfn is retained in a Rab22a-containing compartment that does not tubulate with brefeldin A. TRVb-1 cells expressing GFP (A to C), GFP-cRab22aWT (D to F), GFP-hRab4aWT (J), GFP-human cellubrevin (N), or GFP-hRab11aWT (R) were allowed to internalize tetramethylrhodamine-labeled Tfn for 30 min at 37°C in the continuous presence of BfA (5 μg/ml). Cells coexpressing RFP-cRab22aWT and GFP-hRab4aWT (G to I), GFP-human cellubrevin (K to M), or GFP-hRab11aWT (O to Q) received the same treatment but using Alexa Fluor 647-labeled Tfn. Cells were fixed, and fluorescence images were recorded in a confocal microscope. Images (summation of all confocal planes) were merged and aligned using Adobe Photoshop 7.0. Bars, 10 μm.

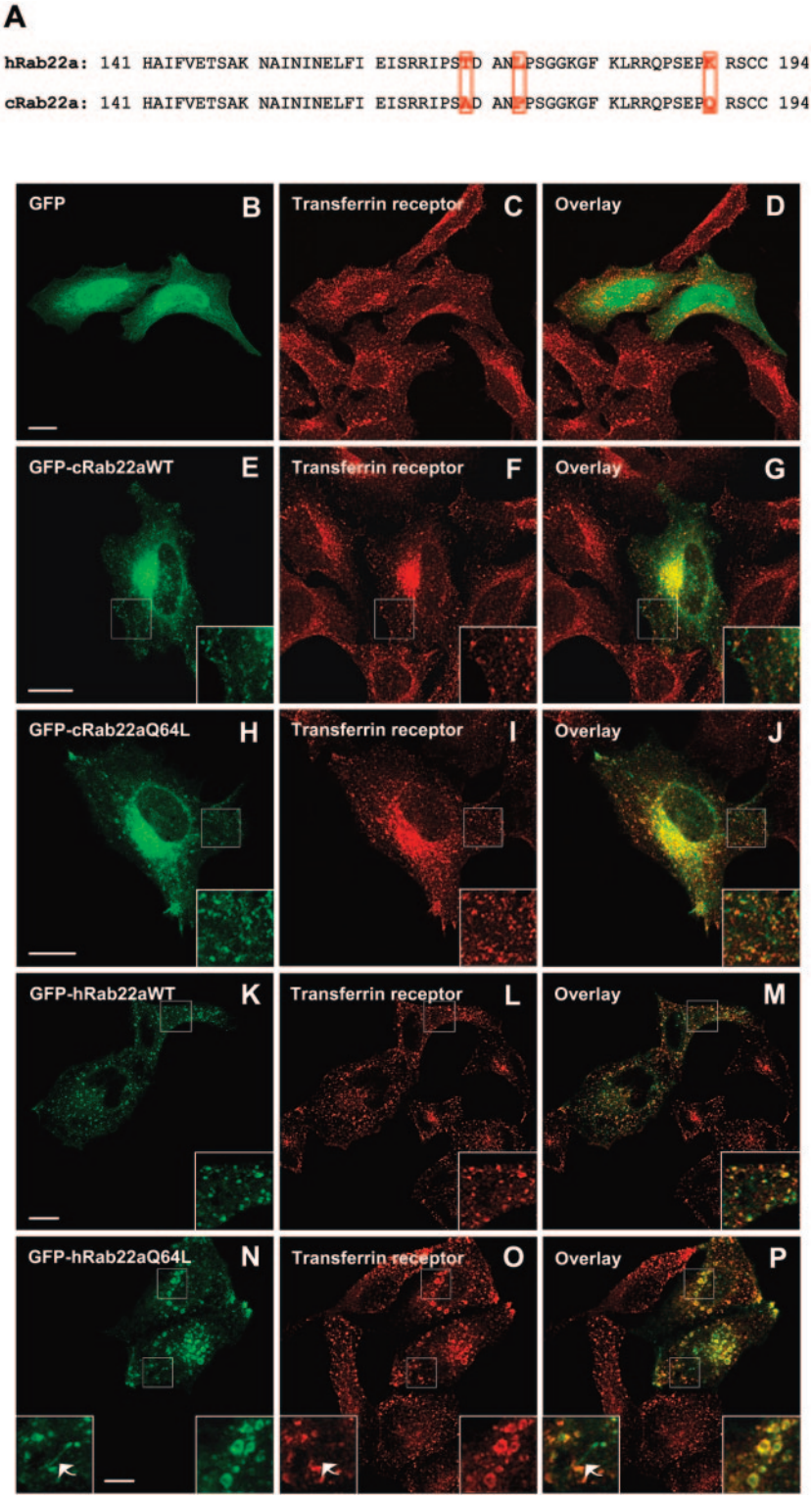

FIG. 10. Expression of canine and human Rab22a differentially affects TfnR subcellular distribution in HeLa cells. The carboxy-terminal sequences of human and canine Rab22a are shown in panel A. Differences between the proteins are labeled in red. HeLa cells were transiently transfected with pEGFP-C1 (B to D), pEGFP-C1-cRab22aWT (E to G), pEGFP-C1-cRab22aQ64L (H to J), pEGFP-C1-hRab22aWT (K to M), or pEGFP-C1-hRab22aQ64L (N to P). Eighteen hours later, the cells were fixed and labeled with a monoclonal anti-human TfnR antibody. The distribution of the fluorescent proteins was recorded in a confocal microscope. Images (summation of all confocal planes) were merged and aligned using Adobe Photoshop 7.0. Bars, 10 μm.

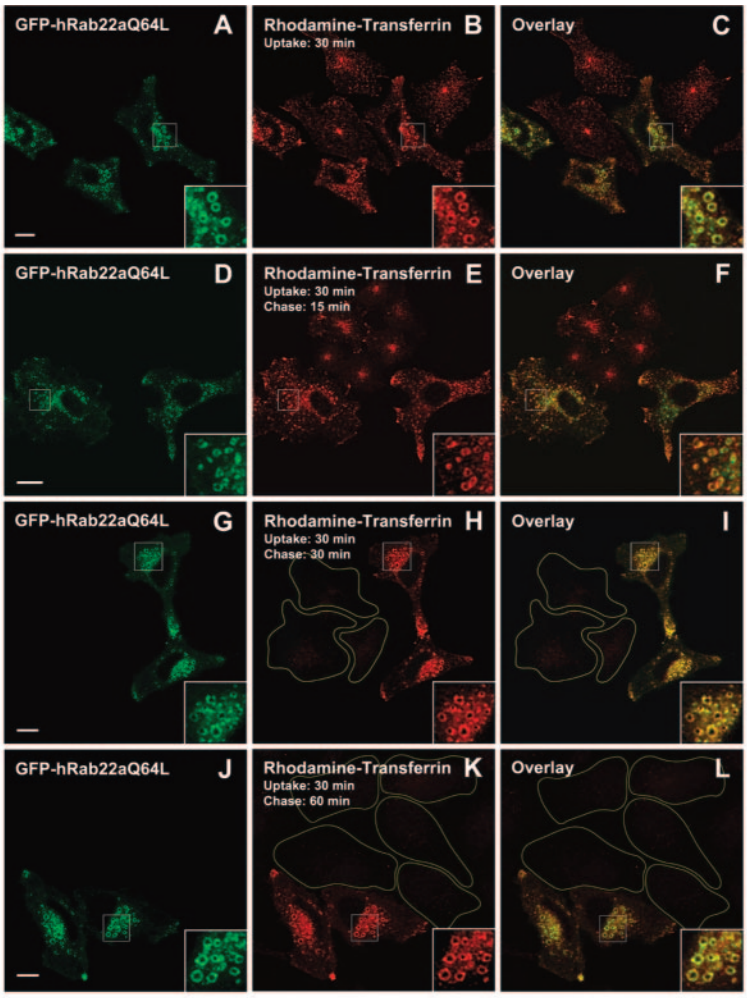

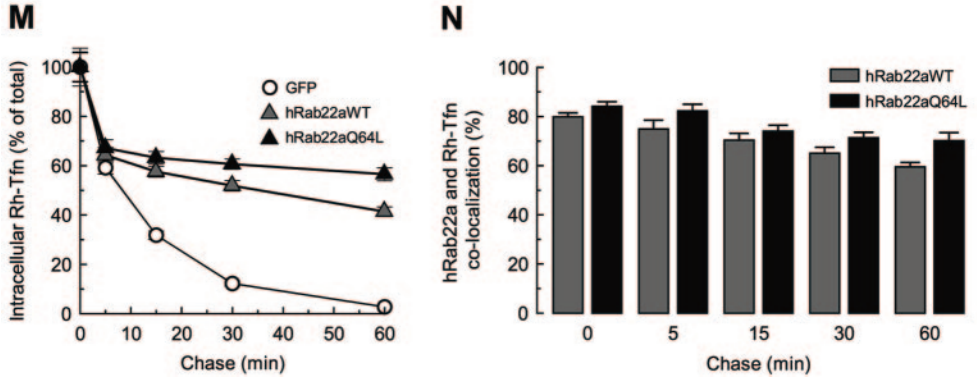

FIG. 11. Expression of human Rab22a inhibits the recycling of Tfn in HeLa cells. HeLa cells transfected with pEGFP-C1, pEGFP-C1-hRab22aWT, or pEGFP-C1-hRab22aQ64L were incubated for 30 min at 37°C with tetramethylrhodamine-labeled Tfn. The cells were then washed and incubated in medium containing an excess of unlabeled Tfn for 0, 5, 15, 30, or 60 min at 37°C. Cells were fixed, and the distribution of the fluorescent proteins was recorded in a confocal microscope. After a 30-min uptake, untransfected and transfected cells presented intense Tfn labeling. However, in untransfected cells (B), Tfn accumulated in the recycling center and in small vesicles throughout the cytoplasm. In contrast, in cells expressing hRab22aQ64L, Tfn localized in large hRab22a-containing endosomes in the periphery of the cell (A to C). When cells were chased for 30 or 60 min, Tfn disappeared from untransfected cells (silhouettes in panels H and K). However, cells expressing hRab22aQ64L retained Tfn in hRab22a-positive compartments (D to L). Images (summation of all confocal planes) were merged and aligned using Adobe Photoshop 7.0. Bars, 10 μm. Quantification of the morphological data for cells expressing GFP (white circles), GFP-hRab22aWT (gray triangles), or GFP-hRab22aQ64L (black triangles) is shown in panel M. hRab22a-positive structures retain Tfn throughout the chase period in cells expressing GFP-hRab22aWT (gray bars) or GFP-hRab22aQ64L (black bars) (N). The data in panels M and N represent the means ± standard errors of the means from three independent experiments quantified as summarized in Materials and Methods.

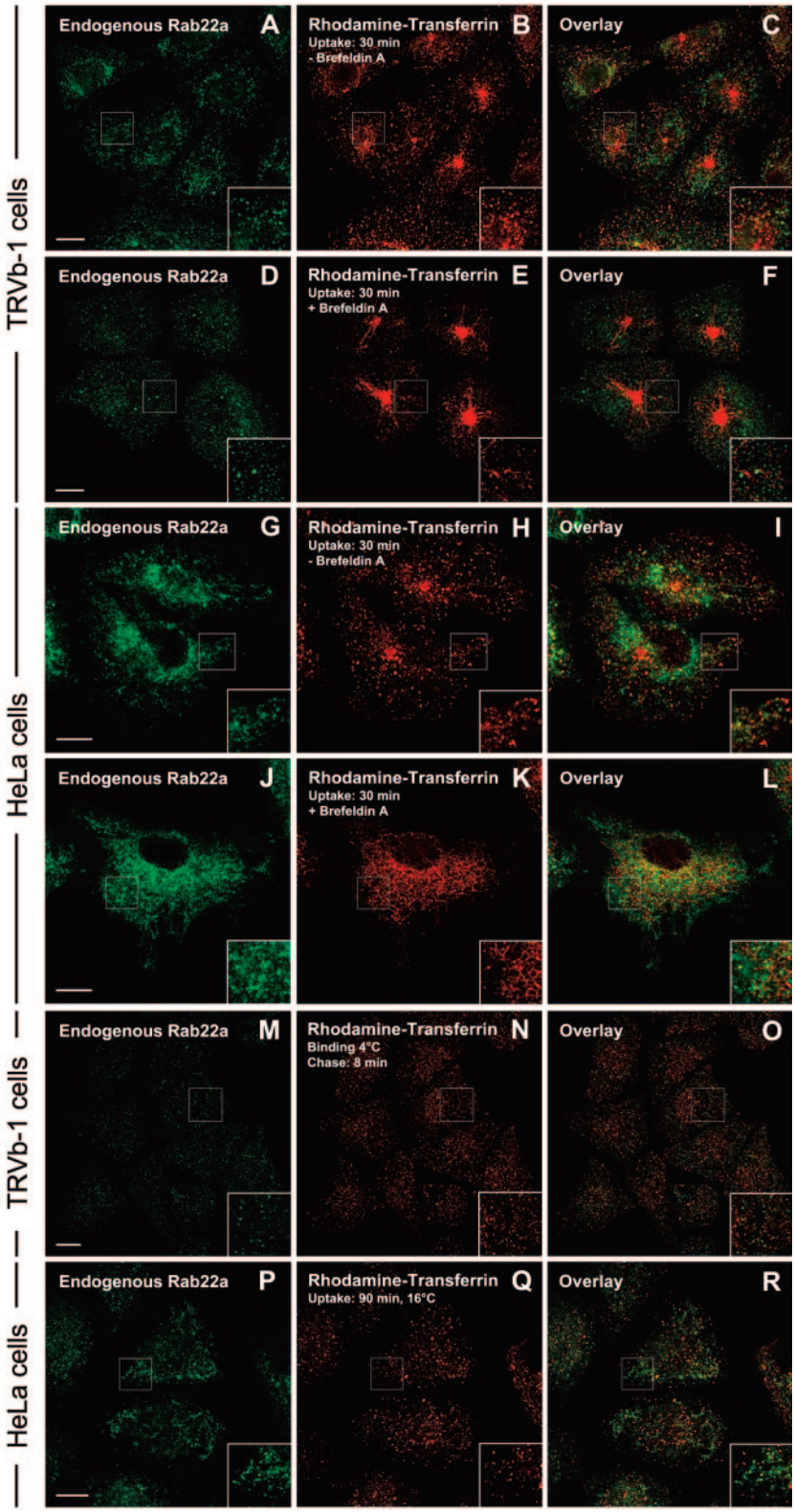

FIG. 12. Distribution of endogenous Rab22a in CHO and HeLa cells. In TRVb-1 (A to F and M to O) or HeLa (G to L and P to R) cells, tetramethylrhodamine-labeled Tfn was internalized for 30 min at 37°C (A to L) in the presence (D to F and J to L) or absence (A to C and G to I) of BfA (5 μg/ml), bound at 4°C and internalized for 8 min at 37°C (M to O), or internalized at 16°C for 90 min (P to R). At the end of the incubation, cells were fixed and immunolabeled with an affinity-purified anti-Rab22a antibody (see Fig. S3 in the supplemental material). Fluorescence images were recorded in a confocal microscope. Images (summation of all confocal planes) were merged and aligned using Adobe Photoshop 7.0. Bars, 10 μm.

Rab22a depletion by siRNA affects Tfn recycling in HeLa cells. Tfn enters into Rab22a-positive structures along its intracellular route, and overexpression of Rab22a profoundly alters the Tfn pathway. We wondered whether endogenous Rab22a plays an active role in the transport of this protein. To address this point, HeLa cells were transfected with pSuper.gfp/neo vector with a sequence directed against hRab22a (28). Transfected cells were identified by the expression of GFP. In these cells, immunofluorescence against the endogenous Rab22a was strongly reduced (see Fig. S4 in the supplemental material), indicating that the expression of the protein was inhibited by the siRNA. No effect was observed when cells were transfected with pSuper.gfp/neo vector encoding a scrambled siRNA (see Fig. S4 in the supplemental material). In cells with low levels of endogenous Rab22a, the TfnR was distributed in vesicles scattered in the cytoplasm. The perinuclear recycling center (present in cells transfected with scrambled siRNA) was not observed (compare Fig. 13A and B). Consistent with these observations, after a 30-min continuous uptake, Tfn localized preferentially in peripheral vesicles, and the recycling center was disorganized (compare Fig. 13C and D). The number of cells with well-organized perinuclear recycling centers was reduced from 75% to 80% in untransfected cells or cells expressing an irrelevant siRNA to 25% in cells with low levels of Rab22a (Fig. 13H). When cells were incubated with an excess of unlabeled Tfn after the 30-min uptake, recycling was significantly reduced in Rab22a-depleted cells (compare Fig. 13E and F). Note that Tfn was retained in small vesicles in the periphery of the cell and never arrived to the perinuclear region (Fig. 13F). A quantification of the images showed that all cells recycled approximately the same amount of Tfn during the first few minutes. However, about 50% of the internalized protein remained cell associated after 60 min of chase in cells expressing the hRab22a siRNA, whereas it was almost completely recycled in untransfected cells or cells expressing scrambled siRNA (Fig. 13G). These observations indicate that Rab22a actively participates in the intracellular transport of Tfn, likely in the step between sorting and recycling endosomes.

DISCUSSION

Tfn is transported in most cells through a well-defined recycling pathway. Diferric Tfn binds to the TfnR on the cell surface, is internalized in coated vesicles, and is delivered to sorting endosomes. At the mildly acidic pH of this compartment, the iron is released from the protein and the TfnR, together with apo-Tfn, is recycled directly to the plasma membrane or transported to the recycling endosomes, from which they are delivered to the cell surface (10). This pathway is shared for several integral membrane proteins that are transported in and out of the cell surface hundreds of times during their life span, avoiding being digested in late endocytic compartments. Several Rabs are important for Tfn intracellular transport. Rab5 is a key element for transport between the plasma membrane and sorting endosomes and for homotypic fusion among endosomes. Rab4 is necessary for the efficient recycling from sorting and recycling endosomes (5, 24, 27). Rab11 participates in the secretory and recycling pathways (3, 19). In the recycling pathway, it plays a role distal to Rab4, likely in the fusion of vesicles with the plasma membrane (24, 27). Results from several laboratories indicate that, in addition to Rab5, Rab4, and Rab11, several other members of the Rab family are important for Tfn intracellular transport. Expression of Rab15WT and the Q67L mutant in TRVb-1 cells inhibits Tfn internalization but does not affect Tfn receptor recycling, suggesting that this Rab behaves as a negative regulator for Tfn uptake (30). Upon transfection of HeLa cells with Rab14Q70L, a fraction of each cell's TfnR is shifted from the TGN toward a peripheral localization, favoring a role of Rab14 in TGN-to-early endosome transport (8). In the same cell line, expression of Rab21T33N decreases Tfn uptake, suggesting that this Rab is also involved in early steps of endocytosis (23).

Expression of cRab22aWT or cRab22aQ64L in CHO cells causes a strong effect on the Tfn pathway. TfnRs are depleted from the cell surface and accumulate in cRab22a-positive compartments in the periphery of the cell. Quantitative analysis of radioactive and fluorescent Tfn uptake indicates that the kinetics of internalization was not affected. However, a large percentage of Tfn was trapped inside the cell. The effect was notable only for chase periods longer than 15 min, indicating that recycling from early compartments was not significantly retarded. The intracellular transport of Tfn has been modeled in CHO cytoplasts microsurgically created (21). The model considers two intracellular endocytic compartments: E1 (early endosomes) and E2 (recycling endosomes), from which Tfn can be recycled to the cell surface. The kinetic constants for internalization and recycling adjusted to our results are comparable to those reported previously. In CHO cells expressing cRab22aWT or the Q64L mutant, the kinetics of transport from the plasma membrane to E1 and from E1 back to the cell surface were not strongly affected by the expression of cRab22a. In contrast, transport from E2 to E1 or to the cell surface was dramatically reduced. Therefore, E2 behaves as a sink in which Tfn is trapped. The morphological observation that Tfn in these cells colocalizes with cRab22a indicates that E2 is a cRab22a-positive compartment. No colocalization was observed with several late endosome/lysosome markers, indicating that Tfn was not routed to lysosomes. Indeed, markers internalized by fluid phase (dextran and horseradish peroxidase) (12, 13) or receptor-mediated endocytosis (epidermal growth factor and Tfn) (9, 12) arrive at the large cRab22a-labeled compartments after short periods of time (≅5 min) (Fig. 3 and 5). They are also positive for EEA1, Rab5a, and Rab4a (Fig. 2 and 8) (see Fig. S1 in the supplemental material) (9). All this evidence indicates that E2 is an early endocytic compartment. TfnR and cellubrevin, two proteins that normally localize in recycling endosomes, were also redistributed to peripheral cRab22a-positive compartments. Only Rab11a conserved most of its perinuclear localization; although, at high cRab22a expression levels, it was also found preferentially in cRab22a-positive compartments. BfA, which is known to tubulate recycling endosomes, did not change the morphology of cRab22a-positive structures. Interestingly, in cells coexpressing cRab22aWT and Rab4a or cellubrevin, these proteins, which normally localize to BfA-sensitive compartments, were redistributed to BfA-resistant, cRab22a-positive structures. The results indicate that many markers of sorting endosomes and recycling endosomes are retained in enlarged cRab22a-positive endosomes that probably correspond to the

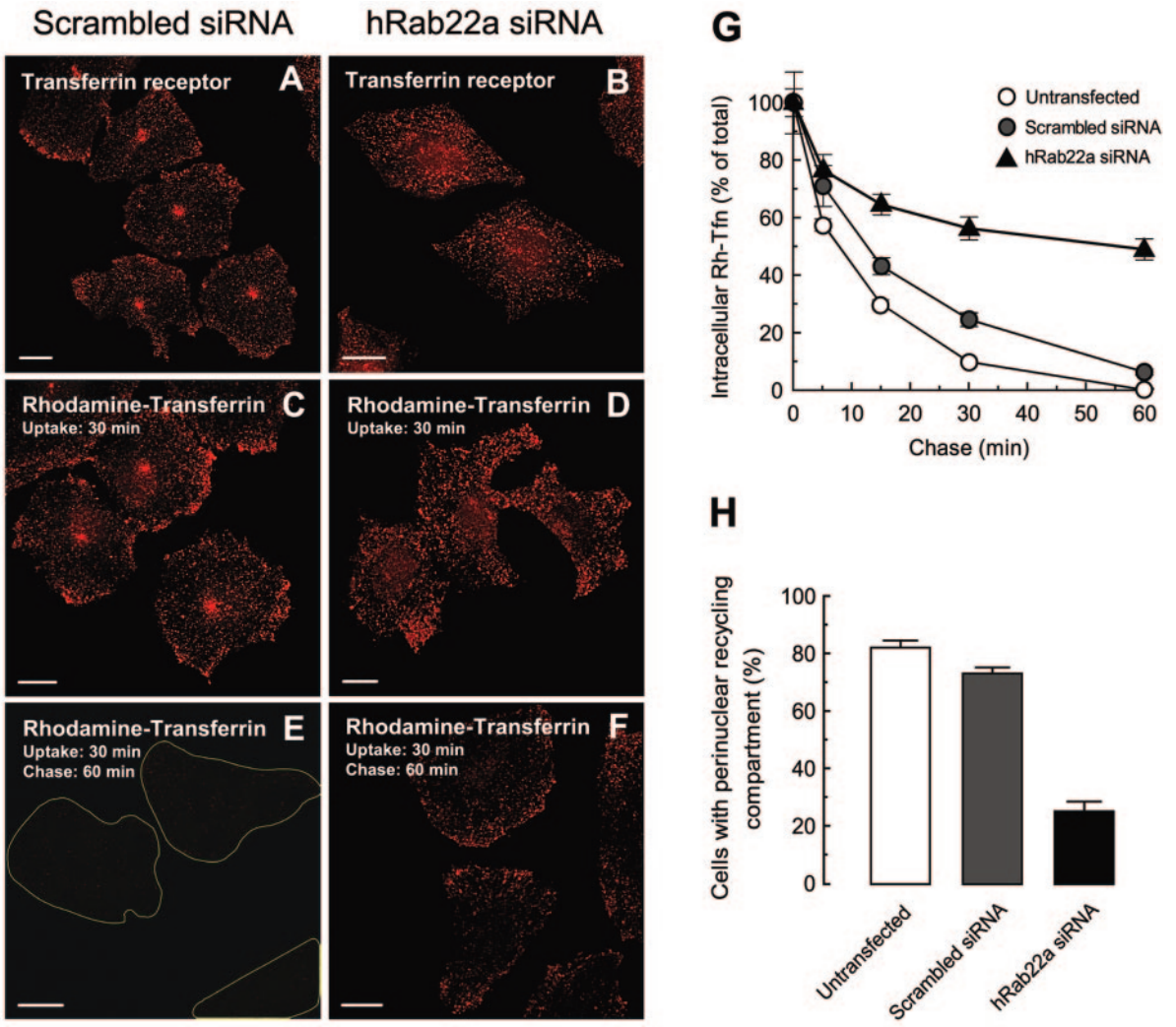

FIG. 13. Knockdown of endogenous Rab22a alters Tfn recycling in HeLa cells. HeLa cells transfected with pSuper.gfp/neo-scrambled siRNA (A, C, and E) or with pSuper.gfp/neo-human Rab22a siRNA (B, D, and F) were grown for 6 days in the presence of 400 μg/ml G-418. Transfected and untransfected cells were fixed and immunostained with an anti-TfnR antibody. Alternatively, the cells were first incubated for 30 min at 37°C with tetramethylrhodamine-labeled Tfn and then washed and incubated in medium containing an excess of unlabeled Tfn for 0, 5, 15, 30, or 60 min at 37°C. Cells were fixed, and the distribution of the fluorescent proteins was recorded in a confocal microscope. Images (summation of all confocal planes) were merged and aligned using Adobe Photoshop 7.0. Bars, 10 μm. siRNA for Rab22a altered the subcellular localization of TfnR (compare panels A and B) and Tfn (30-min uptake, 0-min chase) (compare panels C and D). A substantial amount of Tfn was retained in these cells after a 60-min chase (compare panels E and F). All cells shown in panels A to F expressed GFP (data not shown), indicating that untransfected cells were efficiently eliminated by selection in the presence of G-418. Quantification of the amount of cell-associated Tfn for untransfected cells (white circles) or cells expressing scrambled siRNA (gray circles) or Rab22a-specific siRNA (black triangles) was performed as summarized in Materials and Methods and shown in panel G. Cells with a well-defined perinuclear recycling center (labeled by a 30-min continuous uptake of Tfn) were counted using a regular fluorescence microscope (at least 350 cells in 35 different fields were classified for each condition) and expressed as a percentage of the total number of cells analyzed (white, gray, and black bars represent untransfected, scrambled siRNA, and hRab22a-specific siRNA groups, respectively) (H). The data in panels G and H represent the means ± standard errors of the means from three independent experiments.

E2 compartment defined by kinetic studies. In contrast, wild-type cRab22a does not affect the morphology and function of late endocytic structures. This protein is excluded from compartments enriched in human Rab7 (12), LysoTracker Red, or cathepsin D (Fig. 8).

In HeLa cells, cRab22a participates in the recycling of MHC-I (28). MHC-I is internalized in nonclathrin-coated vesicles and recycled through a different pathway than Tfn in this cell line (16). It has been reported that expression of different mutants of canine Rab22a does not alter Tfn recycling in HeLa cells (9, 28), a result that is consistent with our own observations (Fig. 10). However, when the human Rab22a wild type or the GTPase-deficient mutant are replaced by the canine proteins, Rab22a-expressing cells showed altered distribution of the TfnR and impaired Tfn recycling (Fig. 11). These observations suggest that the minor differences between the canine and human Rab22a present in the carboxy-terminal domain are recognized by some Rab22a-interacting proteins in the human cell line. The dissimilar effects of human and canine Rab22a in HEK 293 and Vero cells were also observed (see

Fig. S2 in the supplemental material). Some highly homologous Rab proteins can interact with different proteins. For example, Rab6A and Rab6A′ differ in only three amino acids and have different effectors and function within the same cell (6). As described for the canine protein (28), we observed that hRab22a also labels Tfn-negative tubules that have been implicated in MHC-I transport, suggesting that the canine protein interacts correctly with effectors in this pathway.

Our results with overexpressed proteins are consistent with a role for Rab22a in the intracellular transport of Tfn. This methodological approach has been used extensively to characterize the role of most Rabs in membrane transport; however, overexpression may introduce several artifacts, such as mistargeting the protein to other compartments, altering the steady-state condition of intracellular pathways, and affecting the function of other Rabs by cross talking between Rab-interacting proteins (e.g., GAPs, GEFs, and common effectors). To address these problems, we have localized the endogenous Rab22a and assessed the effect of depletion of this protein by siRNA. Our results show a significant colocalization between Tfn and endogenous Rab22a in early/sorting endosomes in both TRVb-1 and HeLa cells (Fig. 12). Very little endogenous Rab22a was present in the recycling center. Rab22a was also present in tubular structures—especially prominent in HeLa cells—that were depleted of Tfn and may correspond to compartments involved in MHC-I transport (28). Depletion of endogenous Rab22a by siRNA using a previously described human sequence (28) disorganized the perinuclear recycling center. More importantly, this treatment caused a 50% inhibition of Tfn recycling (Fig. 13). This is a very strong effect for a protein that can recycle directly from early/sorting endosomes, a process that, according to our results, is not affected by Rab22a overexpression or depletion. A similar level of inhibition is obtained by overexpressing the dominant-negative mutant of Rab11, a well-known Rab involved in Tfn recycling. Weigert et al. have shown that siRNA with the same human sequence for Rab22a significantly diminishes the recycling of Tfn and strongly reduces the recycling of MHC-I (28). Although those authors concluded that Rab22a is active only in the recycling of MHC-I, our interpretation of their and our data is that this GTPase is involved in both pathways. In conclusion, the experiments with overexpressed proteins, endogenous Rab22a, and Rab22a depletion indicate that Rab22a plays an important role in the intracellular transport of Tfn in many cells.

We favor the idea that Rab22a controls the exit from sorting endosomes. Previously, we have shown that in CHO cells, the expression of cRab22aWT or cRab22aQ64L retains in modified sorting endosomes macromolecules that are transported to the TGN (e.g., cation-independent mannose-6-phosphate receptor and cholera toxin) (12). Now, we report that in cells with abnormal (high or low) levels of Rab22a, Tfn is normally internalized from the cell surface and directed to functional early endosomes from which it can recycle back to the cell surface. These endosomes may represent very early compartments, with low Rab22a concentrations, that can normally recruit and segregate Rab4-enriched domains that will pinch off and recycle material to the plasma membrane. Eventually, these structures will fuse with Rab22a-positive endosomes. In cells overexpressing Rab22a, transport out of these modified endosomes is probably delayed by enhanced homotypic fusion that would prevent the segregation of membrane domains capable of interacting with a different compartment (18, 20, 29). Therefore, these enlarged endosomes will accumulate Tfn bound to its receptor and other membrane proteins involved in recycling and retrograde transport to the TGN (9, 12). In cells with Rab22a depleted, the transport to perinuclear recycling endosomes is delayed and Tfn is retained in sorting endosomes. These cells may have also impaired the recycling of other molecules, such as MHC-I. In brief, Rab22a is emerging as an important factor involved in the sorting of a large set of macromolecules that are transported to different intracellular destinations.

ACKNOWLEDGMENTS

This work was partly supported by an International Research Scholar Award from the Howard Hughes Medical Institute and by a grant from ANPCyT, Argentina, to L.S.M. and by NIH GM 042259 and the NSF U.S.-Argentina Cooperative Research Award to P.D.S. J.G.M. is a CONICET fellow (Argentina) and has received support from IUBMB and the *Journal of Cell Science* for training visits to the P.D.S. laboratory.

We thank E. Peters, A. Medero, and M. Furlán for excellent technical assistance, J. Gruenberg and W. Brown for antibodies, and M. Zerial, I. Mellman, M. I. Colombo, and T. Galli for plasmids. We thank M. I. Colombo and M. T. Damiani for critical reading of and helpful comments on the manuscript.

REFERENCES

1. **Brummelkamp, T. R., R. Bernards, and R. Agami.** 2002. A system for stable expression of short interfering RNAs in mammalian cells. Science **296:**550–553.
2. **Bucci, C., R. G. Parton, I. H. Mather, H. Stunnenberg, K. Simons, B. Hoflack, and M. Zerial.** 1992. The small GTPase Rab5 functions as a regulatory factor in the early endocytic pathway. Cell **70:**715–728.
3. **Chen, W., Y. Feng, D. Chen, and A. Wandinger-Ness.** 1998. Rab11 is required for trans-Golgi network-to-plasma membrane transport and a preferential target for GDP dissociation inhibitor. Mol. Biol. Cell **9:**3241–3257.
4. **Daro, E., P. van der Sluijs, T. Galli, and I. Mellman.** 1996. Rab4 and cellubrevin define different early endosome populations on the pathway of transferrin receptor recycling. Proc. Natl. Acad. Sci. USA **93:**9559–9564.
5. **De Renzis, S., B. Sonnichsen, and M. Zerial.** 2002. Divalent Rab effectors regulate the sub-compartmental organization and sorting of early endosomes. Nat. Cell Biol. **4:**124–133.
6. **Echard, A., F. J. Opdam, H. J. de Leeuw, F. Jollivet, P. Savelkoul, W. Hendriks, J. Voorberg, B. Goud, and J. A. Fransen.** 2000. Alternative splicing of the human Rab6A gene generates two close but functionally different isoforms. Mol. Biol. Cell **11:**3819–3833.
7. **Gruenberg, J., and H. Stenmark.** 2004. The biogenesis of multivesicular endosomes. Nat. Rev. Mol. Cell Biol. **5:**317–323.
8. **Junutula, J. R., A. M. De Maziere, A. A. Peden, K. E. Ervin, R. J. Advani, S. M. van Dijk, J. Klumperman, and R. H. Scheller.** 2004. Rab14 is involved in membrane trafficking between the Golgi complex and endosomes. Mol. Biol. Cell **15:**2218–2229.
9. **Kauppi, M., A. Simonsen, B. Bremnes, A. Vieira, J. Callaghan, H. Stenmark, and V. M. Olkkonen.** 2002. The small GTPase Rab22 interacts with EEA1 and controls endosomal membrane trafficking. J. Cell Sci. **115:**899–911.
10. **Maxfield, F. R., and T. E. McGraw.** 2004. Endocytic recycling. Nat. Rev. Mol. Cell Biol. **5:**121–132.
11. **McGraw, T. E., L. Greenfield, and F. R. Maxfield.** 1987. Functional expression of the human transferrin receptor cDNA in Chinese hamster ovary cells deficient in endogenous transferrin receptor. J. Cell Biol. **105:**207–214.
12. **Mesa, R., J. Magadán, A. Barbieri, C. López, P. D. Stahl, and L. S. Mayorga.** 2005. Overexpression of Rab22a hampers the transport between endosomes and the Golgi apparatus. Exp. Cell Res. **304:**339–353.
13. **Mesa, R., C. Salomón, M. Roggero, P. D. Stahl, and L. S. Mayorga.** 2001. Rab22a affects the morphology and function of the endocytic pathway. J. Cell Sci. **114:**4041–4049.
14. **Motulsky, H. J., and L. A. Ransnas.** 1987. Fitting curves to data using nonlinear regression: a practical and nonmathematical review. FASEB J. **1:**365–374.
15. **Murray, J. W., and A. W. Wolkoff.** 2003. Roles of the cytoskeleton and motor proteins in endocytic sorting. Adv. Drug Delivery Rev. **55:**1385–1403.

16. **Naslavsky, N., R. Weigert, and J. G. Donaldson.** 2003. Convergence of non-clathrin- and clathrin-derived endosomes involves Arf6 inactivation and changes in phosphoinositides. Mol. Biol. Cell **14:**417–431.
17. **Novick, P., and M. Zerial.** 1997. The diversity of Rab proteins in vesicle transport. Curr. Opin. Cell Biol. **9:**496–504.
18. **Pfeffer, S.** 2003. Membrane domains in the secretory and endocytic pathways. Cell **112:**507–517.
19. **Ren, M., G. Xu, J. Zeng, C. De Lemos-Chiarandini, M. Adesnik, and D. D. Sabatini.** 1998. Hydrolysis of GTP on Rab11 is required for the direct delivery of transferrin from the pericentriolar recycling compartment to the cell surface but not from sorting endosomes. Proc. Natl. Acad. Sci. USA **95:**6187–6192.
20. **Rink, J., E. Ghigo, Y. Kalaidzidis, and M. Zerial.** 2005. Rab conversion as a mechanism of progression from early to late endosomes. Cell **122:**735–749.
21. **Sheff, D., L. Pelletier, C. B. O'Connell, G. Warren, and I. Mellman.** 2002. Transferrin receptor recycling in the absence of perinuclear recycling endosomes. J. Cell Biol. **156:**797–804.
22. **Shin, H. W., N. Morinaga, M. Noda, and K. Nakayama.** 2004. BIG2, a guanine nucleotide exchange factor for ADP-ribosylation factors: its localization to recycling endosomes and implication in the endosome integrity. Mol. Biol. Cell **15:**5283–5294.
23. **Simpson, J. C., G. Griffiths, M. Wessling-Resnick, J. A. Fransen, H. Bennett, and A. T. Jones.** 2004. A role for the small GTPase Rab21 in the early endocytic pathway. J. Cell Sci. **117:**6297–6311.
24. **Sonnichsen, B., S. De Renzis, E. Nielsen, J. Rietdorf, and M. Zerial.** 2000. Distinct membrane domains on endosomes in the recycling pathway visualized by multicolor imaging of Rab4, Rab5, and Rab11. J. Cell Biol. **149:**901–914.
25. **Stahl, P. D., and M. A. Barbieri.** 2002. Multivesicular bodies and multivesicular endosomes: the "ins and outs" of endosomal traffic. Sci. STKE **141:**pe32.
26. **Ullrich, O., S. Reinsch, S. Urbe, M. Zerial, and R. G. Parton.** 1996. Rab11 regulates recycling through the pericentriolar recycling endosome. J. Cell Biol. **135:**913–924.
27. **Ward, E. S., C. Martinez, C. Vaccaro, J. Zhou, Q. Tang, and R. J. Ober.** 2005. From sorting endosomes to exocytosis: association of Rab4 and Rab11 GTPases with the Fc receptor, FcRn, during recycling. Mol. Biol. Cell **16:**2028–2038.
28. **Weigert, R., A. C. Yeung, J. Li, and J. G. Donaldson.** 2004. Rab22a regulates the recycling of membrane proteins internalized independently of clathrin. Mol. Biol. Cell **15:**3758–3770.
29. **Zerial, M., and H. McBride.** 2001. Rab proteins as membrane organizers. Nat. Rev. Mol. Cell Biol. **2:**107–117.
30. **Zuk, P. A., and L. A. Elferink.** 2000. Rab15 differentially regulates early endocytic trafficking. J. Biol. Chem. **275:**26754–26764.